8

NOTICE: When government or other drawings, specifications or other data are used for any purpose other than in connection with a definitely related government procurement operation, the U. S. Government thereby incurs no responsibility, nor any obligation whatsoever; and the fact that the Government may have formulated, furnished, or in any way supplied the said drawings, specifications, or other data is not to be regarded by implication or otherwise as in any manner licensing the holder or any other person or corporation, or conveying any rights or permission to manufacture, use or sell any patented invention that may in any way be related thereto.

BRL

MEMORANDUM REPORT NO. 1357
JUNE 1961

DETERMINATION OF ORBITAL ELEMENTS AND REFRACTION EFFECTS FROM SINGLE PASS DOPPLER OBSERVATIONS

R. B. Patton, Jr.
V. W. Richard

61-4-6
NOX

Department of the Army Project No. 503-06-011
Ordnance Management Structure Code No. 5210.11.143

BALLISTIC RESEARCH LABORATORIES
ABERDEEN PROVING GROUND, MARYLAND

BALLISTIC RESEARCH LABORATORIES

MEMORANDUM REPORT NO. 1357

JUNE 1961

DETERMINATION OF ORBITAL ELEMENTS AND REFRACTION EFFECTS FROM SINGLE PASS DOPPLER OBSERVATIONS

R. B. Patton, Jr.
V. W. Richard

Ballistic Measurements Laboratory

Presented at the Symposium on Space Research, Florence, Italy, April 1961

Department of the Army Project No. 503-06-011
Ordnance Management Structure Code No. 5210.11.143

ABERDEEN PROVING GROUND, MARYLAND

BALLISTIC RESEARCH LABORATORIES

MEMORANDUM REPORT NO. 1357

HBPatton,Jr./WWRichard/sec
Aberdeen Proving Ground, Md.
June 1961

DETERMINATION OF ORBITAL ELEMENTS AND REFRACTION EFFECTS FROM SINGLE PASS DOPPLER OBSERVATIONS

ABSTRACT

This report presents a method for the determination of the orbital elements of a satellite by observing, in the course of a single pass, the Doppler shift in the frequency of a radio signal which is either transmitted or reflected from the satellite. The method of solution consists of applying a series of differential corrections to a compatible set of approximations for the initial position and velocity components. Techniques for determining these approximations with sufficient accuracy to initiate the computation are discussed.

The method was developed for the DOPLOC tracking system which employs a narrow bandwidth, phase-locked, tracking filter. The latter has been designed to minimize random errors in Doppler frequency measurements derived from weak signals transmitted over extreme ranges.

Use is also made of satellite Doppler data to determine the total electron content in the ionosphere. A technique for measuring the dispersive Doppler effect is described. Results of computer runs with actual field data are presented.

INTRODUCTION

A method has been developed for the determination of a complete set of orbital parameters from a few minutes of Doppler data recorded in the course of a single pass of a satellite. The source of the signal may be a transmitter in the satellite or a ground-based transmitter reflecting a signal from the satellite. The latter transmitting system requires more costly and complex equipment but offers reliability, an accurately known transmitter frequency, and a stronger geometry for a more accurate orbital computation when the number of receiving stations is limited.

Since it was desired to develop a rapid, reliable, and moderately accurate method of determining the orbital parameters of a satellite tracked by a Doppler system employing a minimum of receiving stations, emphasis was placed on the development of a solution from single pass observations recorded at from one to three receiving sites. The single pass limitation was considered to present a challenging and worthy problem for which there would be numerous applications if a reasonable solution could be developed.

In the past, Doppler data have been used primarily to measure the slope and time of inflection of the frequency-time curve to obtain slant range and time-of-closest-approach information. This is considered to be only an elemental use of the information in the Doppler data. Single pass observations from one receiver have been demonstrated to contain sufficient information for satellite orbital determinations of sufficient accuracy for many applications.

For example, it may be desirable to know the orbital parameters as quickly as possible after launching a satellite. The orbital parameters of a newly launched satellite could be computed within minutes after the beginning of its free flight. Again, after attempting to deflect or steer a satellite into a different orbit, it may be desirable to know the new orbital parameters within a matter of minutes.

The following sections will discuss the practicality of orbit determinations from Doppler data alone and will indicate limitations as well as the obvious advantages for this conceptually simple technique.

DESCRIPTION OF TRACKING EQUIPMENT AND DATA

Doppler observations consist of recordings of Doppler frequency, as a function of time. Here the Doppler frequency is defined to be the frequency obtained by heterodyning a locally generated signal against the signal received from the satellite followed by a correction for the frequency bias introduced as a result of the difference between the frequency of the local oscillator and that of the signal source. In this report, the Doppler frequency is defined to be negative when the satellite is approaching the receiving site and positive when it is receding. If the Doppler frequency, as defined, is plotted as a function of time, one obtains a curve of the form shown in Figure 1, usually referred to as an "S" curve. The asymmetry of the curve is typical for a tracking system with a ground-based transmitter and a receiver separated by an appreciable distance. Only for a satellite whose orbital plane bisects the base line will the Doppler data produce a symmetrical "S" curve with a reflection system. With a satellite-borne transmitter, the "S" curve is very nearly symmetrical, being modified slightly by the Earth's rotation and the refractive effect of the ionosphere. If continuous observations are made and sampled at frequent intervals, such as one per second, Figure 1 (a) illustrates an analog plot of the data available for computer input. However, with a ground based transmitter it may be necessary to limit the number of observations in order to minimize equipment cost and complexity. For example, it is possible to use only three antenna beams and provide three sections of the "S" curve as shown in Figure 1 (b). Another possibility is the use of a scanning antenna beam to provide discreet observations at regular intervals as shown in Figure 1 (c). Such data could be obtained by an antenna with a thin, fan-shaped beam which scanned the sky repetitively.

The data in any of the forms suggested above may be used readily as input for the computing procedure. Whenever possible, this input consists of the total Doppler cycle count over a variable time interval rather than the Doppler frequency itself (i.e. the area under the curves or areas of curves presented in Figure 1 (a) and 1 (b)).

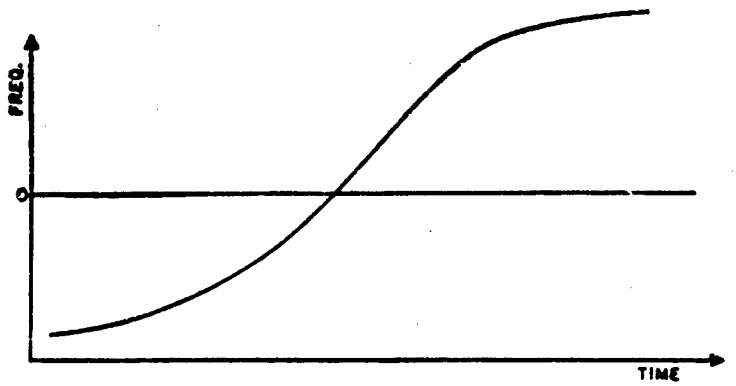

(a)

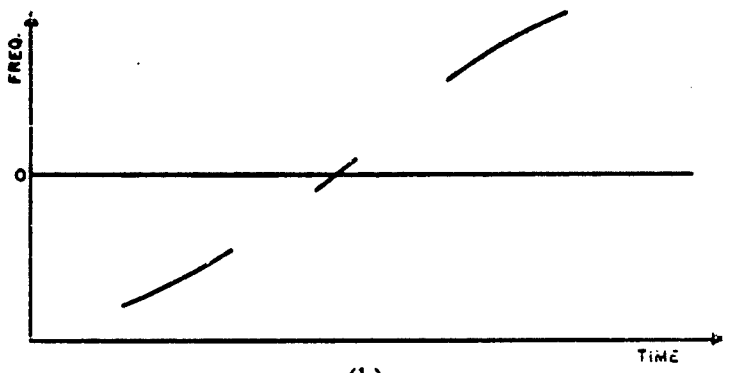

(b)

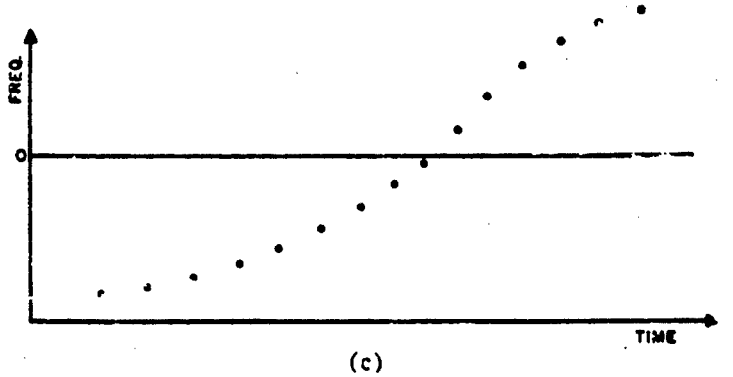

(c)

Fig. 1—Doppler frequency-time curves.

In order to handle the Doppler data rapidly and accurately, the Doppler frequency is automatically counted and digitized at the receiving sites. Figure 2 shows a simplified block diagram of a DOPLOC receiving system. Automatic, real-time counting of the Doppler frequency requires a signal of high quality, that is one with very small random errors introduced by noise. Doppler data, which are essentially noise free, are made possible in the DOPLOC system by use of a very narrow bandwidth, phase-locked, tracking filter (ref. 1) following the receiver. Significant improvements in the signal-to-noise ratio of noisy received signals are realized by extreme reduction of the system bandwidth through the use of the filter. Bandwidths adjustable from 1 to 100 cycles per second are available. The filter is capable of phase-locked operation when a signal is as weak as 36 decibels below the noise, (i.e. a noise-to-signal power ratio of 4000). The filtering action is obtained by use of a frequency-controlled oscillator that is correlated or phase-locked to the input signal. The basic block diagram of the tracking servo loop is shown in Figure 3. Tracking is accomplished with an electronic servo system designed to force the frequency-controlled oscillator to follow the variations of frequency and phase of the input signal. Correlation is maintained with respect to input signal phase, frequency, first time derivative of frequency, and with a finite but small phase error, the second time derivative of frequency. This is done by a cross-correlation detector consisting of the phase detector and filter, or equalizer network. Under dynamic conditions, the control voltage to the oscillator is so filtered in the equalizer network that tracking faithfully reproduces the rate of change of the input frequency. An inherent feature of this design is an effective acceleration memory which provides smooth tracking and extrapolation through signal dropouts. Experience with signal reception from Earth satellites has borne out the necessity for this memory feature, since the received signal amplitude may vary widely and rapidly. The filter works through signal null periods very effectively without losing lock. In addition, this memory provides effective tracking of the desired Doppler signal in the presence of interfering signals when several satellites are within receiving range at the same time.

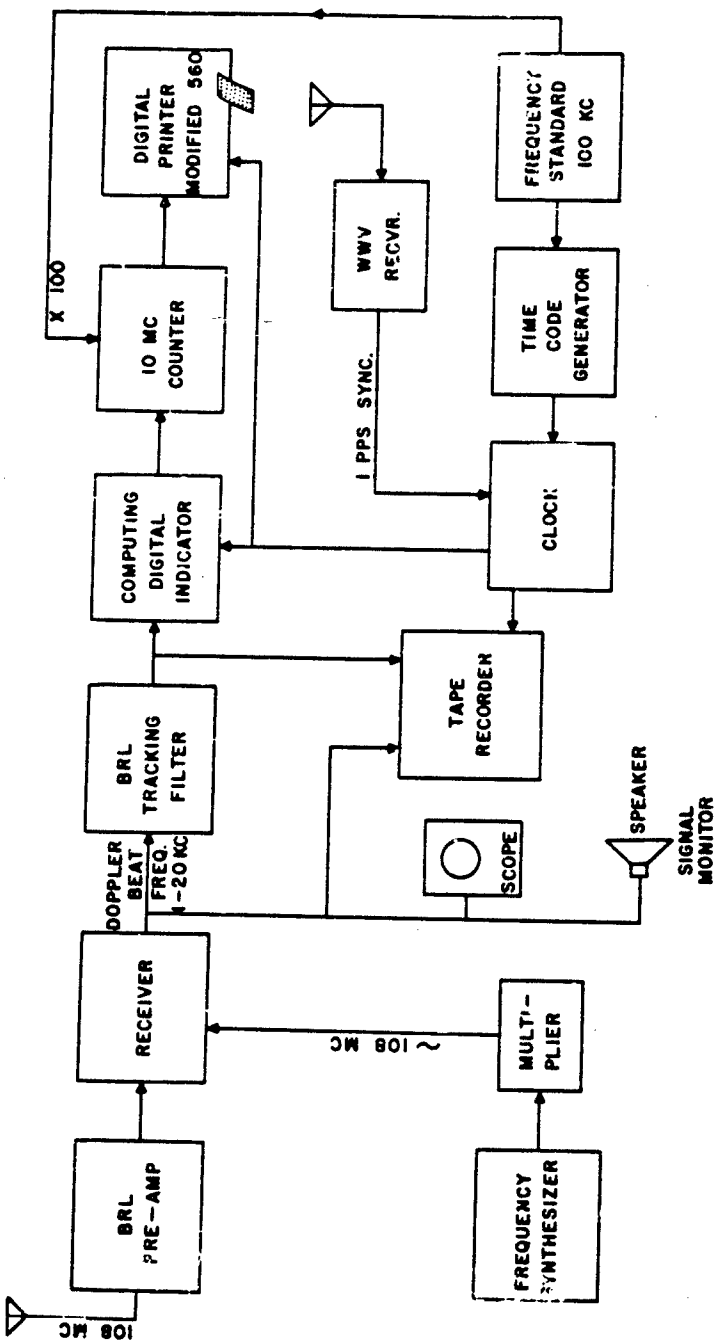

108 MC. DOPLOC STATION
BASIC DOPPLER SATELLITE TRACKING
STATION USING BRL TRACKING FILTER

FIGURE 2

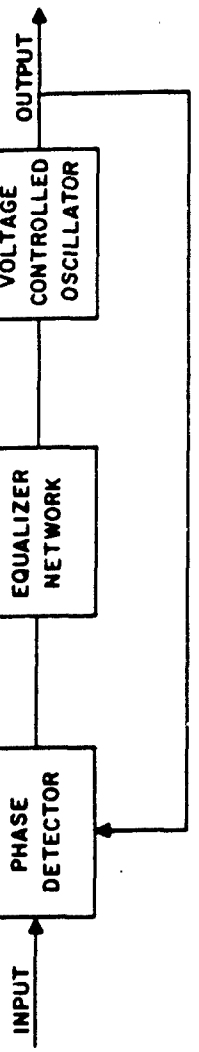

BASIC TRACKING FILTER SYSTEM

FIGURE 3

The signal-to-noise power improvement furnished by the tracking filter is equal to the ratio of the input source noise bandwidth to the filter bandwidth. The internal noise generated by the filter is negligibly small at all bandwidths. The relation between input and output signal-to-noise is shown in Figures 4 and 5. In a typical case with a receiver bandwidth of 10 kc and a filter bandwidth of 5 cps, a signal buried 27 db down in the noise will appear at the filter output with a 6 db signal-to-noise ratio. An experimental investigation (ref. 2) has been made of the relation between signal-to-noise ratio and the uncertainty or random error in measuring the frequency of a Doppler signal. The test results showing R.M.S. frequency error as a function of signal-to-noise ratio and tracking filter bandwidths are shown in Figure 6. For the example cited previously, a signal 27 db down in the noise can be read to an accuracy of 0.15 cps. An integration time or counting time interval of one second was used for these measurements.

The tracking filter can be equipped with a signal search and automatic lock-on system. Signals 30 db down in the noise at typical Doppler frequencies, from 2 to 14 kc, can be detected within a fraction of a second and the filter phase-locked to the signal. With this equipment, signal acquisition and lock-on have become routine in field operations.

The DOPLOC system has been used extensively for satellite tracking. The inherent high sensitivity of the receiving system to signals of very low energy (2×10^{-20} watts, - 197 dbw, or 0.001 microvolts across 50 ohms for a threshold signal at 1 cps bandwidth) has permitted the use of conventional, low gain, wide coverage, antennas to achieve horizon to horizon tracking at great ranges. It has been found to be practical to change bandwidths over the selectable range of 1 to 100 cps in accordance with the information content of the signal and thus achieve maximum signal-to-noise ratio. Since the key to successful determination of orbits lies in obtaining data with small values of random and systematic error, the high quality data output of the DOPLOC system has been an important feature. An orbital solution, developed specifically for this system, has yielded relatively accurate results with a surprisingly small number of DOPLOC tracking observations.

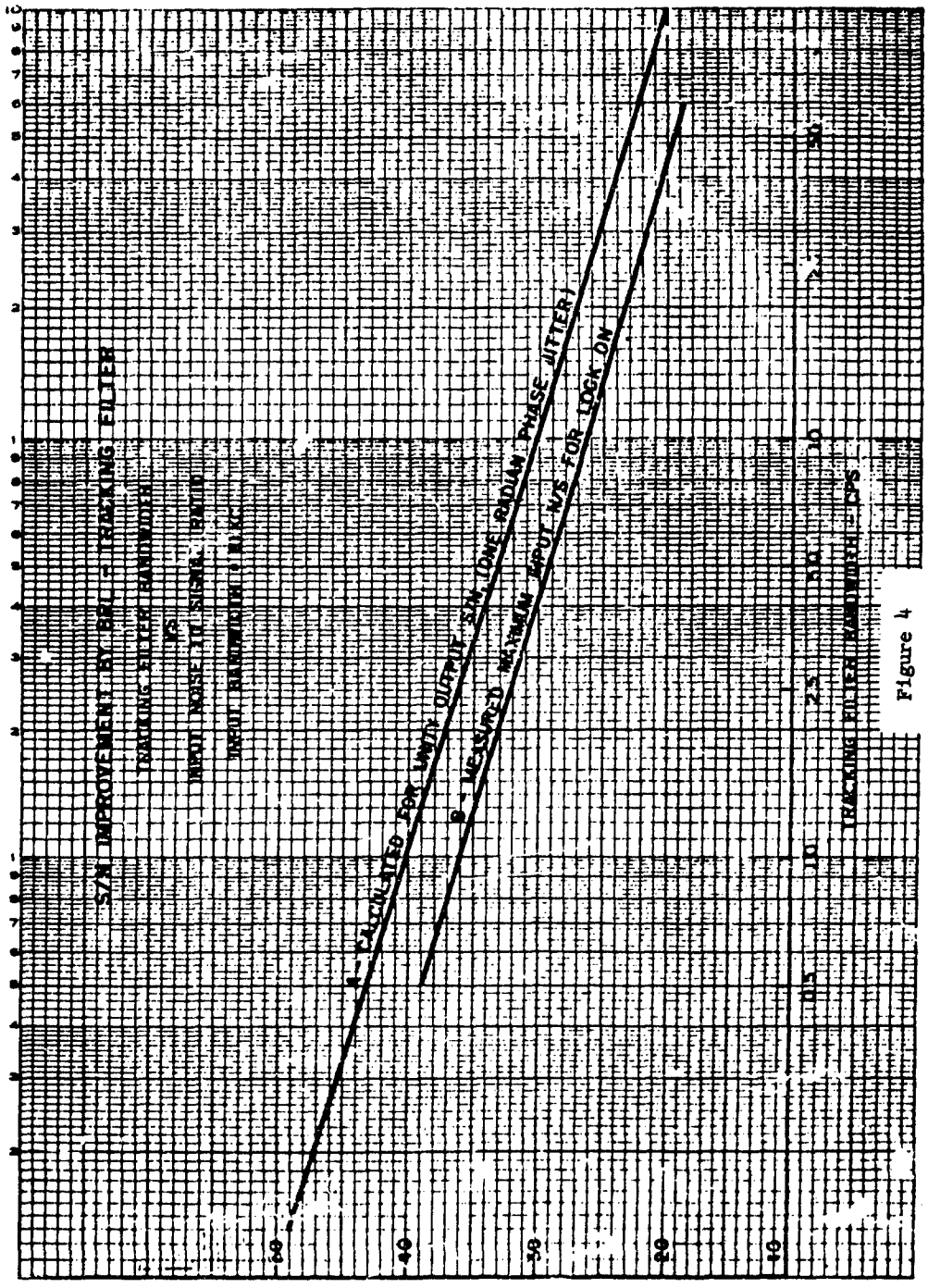
S/N IMPROVEMENT BY BRL - TRACKING FILTER
TRACKING FILTER BANDWIDTH
INPUT NOISE TO SIGNAL RATIO
INPUT BANDWIDTH - B.L.C.
A - CALCULATED FOR UNITY OUTPUT S/N (ONE RADIAN PHASE JITTER)
B - MEASURED MINIMUM INPUT N/S FOR LOCK ON
INPUT NOISE TO SIGNAL RATIO - DB
TRACKING FILTER BANDWIDTH - CPS

Figure 4

INPUT TO FILTER

S/N = 0DB (1:1)
RECEIVER INPUT LEVEL:
8×10^{-17} WATTS, -161 DBW
0.063 MICROVOLTS
ACROSS 50 OHMS

OUTPUT WAVE FORM

+40 DB S/N
0.6° RMS PHASE JITTER

LISSAJOU PATTERN

BETWEEN INPUT AND OUTPUT

INPUT TO FILTER

N/S = 20 DB (100:1 POWER)
RECEIVER INPUT LEVEL:
8×10^{-19} WATTS, -181 DBW
0.0063 MICROVOLTS

OUTPUT WAVE FORM

+20 DB S/N
6° RMS PHASE JITTER

LISSAJOU PATTERN

BETWEEN INPUT AND OUTPUT

INPUT TO FILTER

N/S = 30 DB (1000:1 POWER)
RECEIVER INPUT LEVEL:
8×10^{-20} WATTS, -191 DBW
0.002 MICROVOLTS

OUTPUT WAVE FORM

+10 DB S/N
18° RMS PHASE JITTER

LISSAJOU PATTERN

BETWEEN INPUT AND OUTPUT

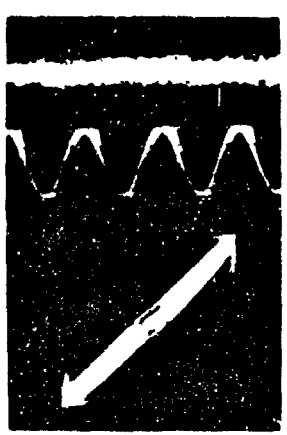

INPUT TO FILTER

N/S = 36 DB (4000 1 POWER)
RECEIVER INPUT LEVEL:
2×10^{-20} WATTS, -197 DBW
0001 MICROVOLTS

OUTPUT WAVE FORM

+4 DB S/N
36° RMS PHASE JITTER

LISSAJOU PATTERN

BETWEEN INPUT AND OUTPUT

INPUT & OUTPUT WAVEFORMS VS NOISE TO SIGNAL RATIO FOR 1 CPS BANDWIDTH

FIGURE 5

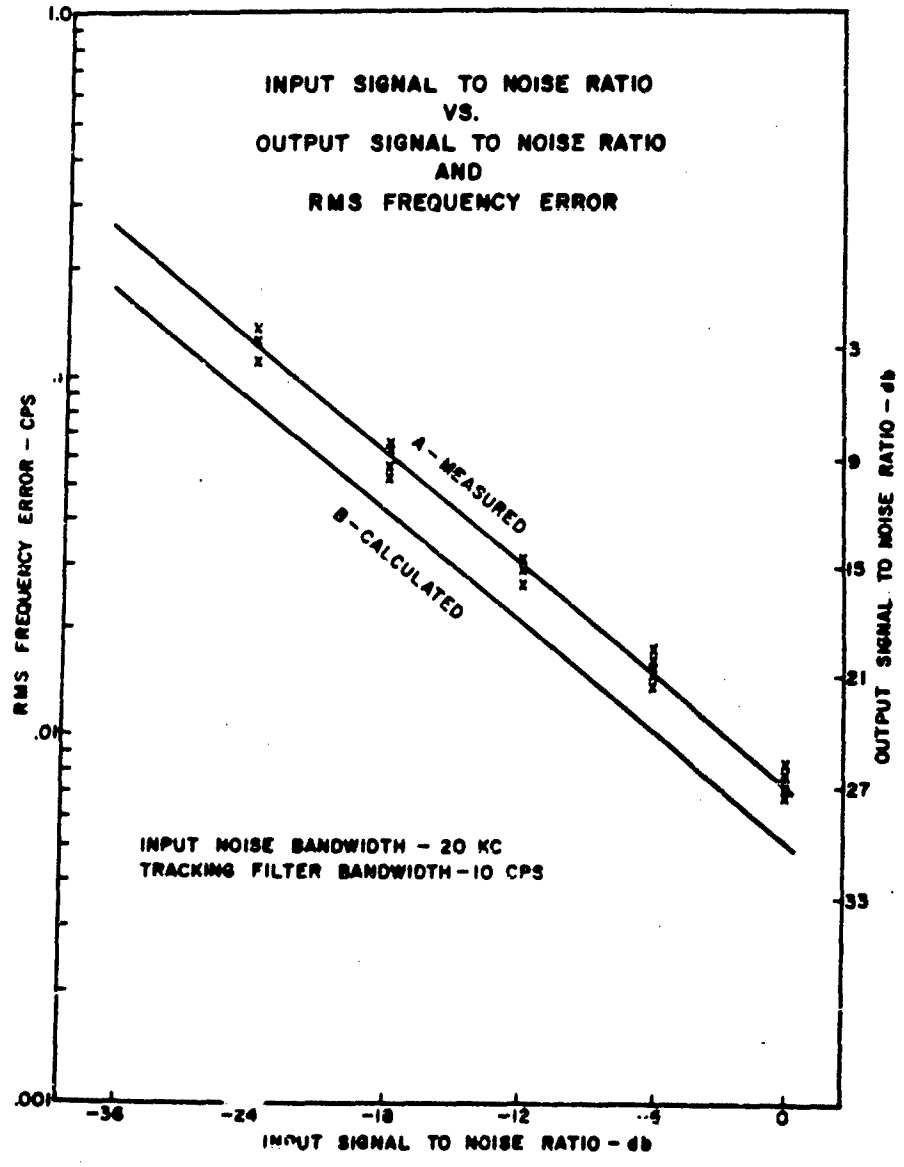
INPUT SIGNAL TO NOISE RATIO
VS.
OUTPUT SIGNAL TO NOISE RATIO
AND
RMS FREQUENCY ERROR
A - MEASURED
B - CALCULATED
INPUT NOISE BANDWIDTH - 20 KC
TRACKING FILTER BANDWIDTH - 10 CPS
RMS FREQUENCY ERROR - CPS
1.0
.01
.001
OUTPUT SIGNAL TO NOISE RATIO - db
3
9
15
21
27
33
-36
-24
-18
-12
-6
0
INPUT SIGNAL TO NOISE RATIO - db

FIGURE 6

THE ORBITAL SOLUTION

The method of solution consists of a curve-fitting procedure, in which a compatible set of approximations for the orbital parameters, are improved by successive differential corrections. The latter are obtained from a least-squares treatment of an over-determined system of equations of condition. The imposed limitation of single pass detection permits several assumptions which considerably simplify the computing procedure. Among these is the assumption that the Earth may be treated dynamically as a sphere while geometrically regarding it as an ellipsoid. In addition, it is assumed that no serious loss in accuracy will result if drag is neglected as a dynamic force. With these assumptions, it is apparent that the satellite may be regarded as moving in a Keplerian orbit. An additional simplification in the reduction of the tracking data is warranted if the frequency of the system exceeds 100 megacycles; for it then becomes feasible to neglect both the atmospheric and ionospheric refraction of the transmitted signal.

In formulating the problem mathematically, it is helpful to regard the instrumentation as an interferometer. In this sense, the total number of Doppler cycles observed within any time interval will provide a measure of the change in slant range from the receiver to the satellite if the transmitter is air-borne, or in the sum of the slant ranges from both the transmitter and receiver to the satellite if the signal originates on the ground and is either reflected or retransmitted by the satellite. Assuming the latter for the discussion which follows, let $g_j(t)$ be defined as the change in the sum of the two slant ranges. It follows from Figure 7 that

$$g_j(t_{12}) = (TS_2 + RS_2) - (TS_1 + RS_1), \qquad (1)$$

where T is the position of the transmitting site, R_j the location of the jth receiver, S_i the position of the satellite at time t_i, and S the

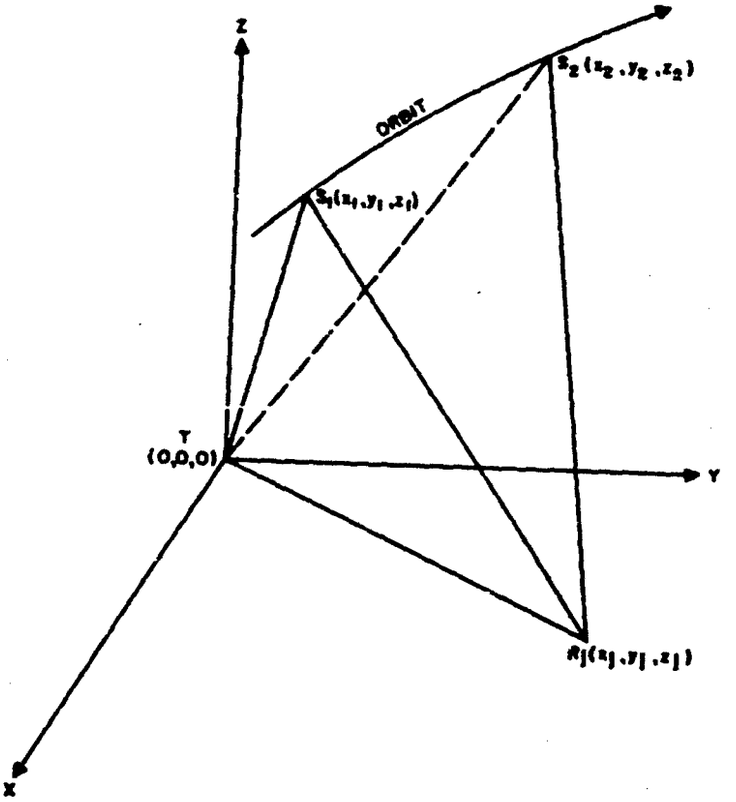

PROBLEM GEOMETRY

FIGURE 7

position at time t_2. $g_j(t_{12})$ is the change in the sum of the slant ranges from the satellite to the transmitter and to the jth receiver in the time interval from t_1 to t_2. It is worth noting that, if this time interval is equal to one second and λ is the wavelength of the transmitted signal, $\left[g_j(t_{12})\right] \div \lambda$ is equivalent to the Doppler frequency for the jth receiver at the time, $(t_1 + 0.5 \text{ sec.})$.

The mathematical development of the computing procedure has been presented in reference 3 and will not be repeated here. Rather, we will confine our remarks to a summary of the more important phases of the method. The solution consists of improving a set of position and velocity components which have been approximated for a specific time. The latter will be defined as t_o and in general, will be within the time interval over which observations have been recorded. The computing procedure is outlined in Figure 8. Initial approximations for position and velocity uniquely define a Keplerian orbit which may be described in terms of the following orbital parameters:

a = semi-major axis,
e = eccentricity,
σ = mean anomaly at epoch,
i = inclination,
Ω = right ascension of the ascending node,
ω = argument of perigee.

After these parameters have been determined, the position of the satellite, and then $g_j(t)$, may readily be computed as a function of time. Comparing the computed values of $g_j(t)$ with the observed values of the same quantity and assuming more than six observations, a set of differential corrections for the initial approximations of position and velocity may then be obtained from a standard least-squares treatment of the resulting over-determined system of equations. The corrections are applied to the initial approximations and the computation is iterated until convergence is achieved.

DIAGRAM OF COMPUTATIONAL PROCEDURE

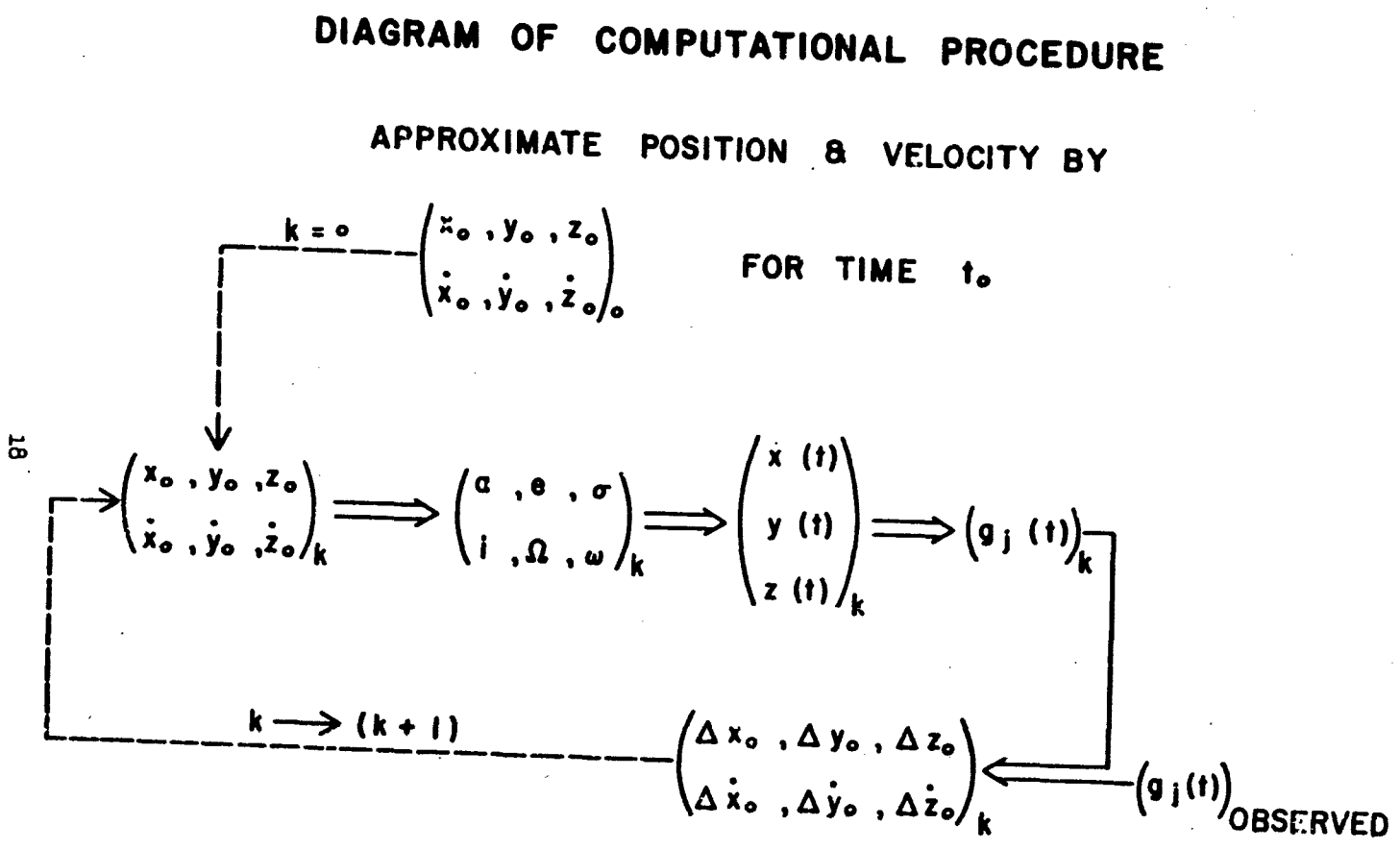

FIGURE 8

This computing procedure essentially determines only those segments of the orbit confined within the intervals of observation. By constraining the satellite to Keplerian motion, the parameters a, e, σ, i, Ω, and ω are likewise determined in the course of the computation; and these serve to provide an estimate of motion over the entire orbit. On the other hand, it has been found impractical to fit an entire ellipse to the observations by solving for the orbital parameters directly.

INITIAL ORBITAL APPROXIMATIONS

Convergence of the computation rests primarily upon the adequacy of the initial approximations for position and velocity. It has been established that, for a system consisting of a single receiver and an earth-bound transmitter at opposite ends of a 400 mile base line, convergence is assured when the error in each coordinate of the initial estimate is not in excess of 50 to 75 miles and the velocity components are correct to within 1/2 to 1 mile per second. When the signal source is carried by the satellite a unique solution is impossible with observations from a single receiver. However, if single pass measurements are available from two or more receivers, with either a ground-based or an air-borne transmitter, the system geometry is greatly strengthened. Convergence can then be expected when the initial approximations are within 150 to 200 miles of the correct value in each coordinate and 1 to 2 miles per second in each velocity component. Larger errors may occasionally be tolerated, but the figures presented are intended to specify limits within which convergence may be reasonably assured.

Therefore, it has been necessary to develop a supporting computation to provide relatively accurate initial approximations to position and velocity for the primary computation. Several successful methods have been developed for this phase of the problem; but discussion will be confined to a few applications of a differential equation derived, in reference 3, to approximately relate the motion of the satellite to the tracking observations. If the transmitter is earth-bound, this equation is of the form

$$\ddot{g}_j = \frac{A - \dot{\rho}_T^2}{\rho_T} + \frac{A - \dot{\rho}_j^2}{\rho_j} , \qquad (2)$$

where the slant ranges from the transmitter and the receiver to the satellite are respectively ρ_T and ρ_j. $\ddot{g}_j$ is the second time derivative of the function defined by equation (1). In deriving equation (2), it was assumed that:

1) in angular measurement, the satellite is within ten degrees of the instrumentation site,
2) the Earth is not rotating,
3) the satellite moves in a circular orbit.

With these assumptions, A may be shown to be approximately equal to $v^4/(GR)$ and hence, constant for a circular orbit since R is the Earth's radius, v is the velocity of the satellite, and G is the mean gravitational constant.

The first application to be considered will be for a system in which the transmitter is carried by the satellite. For the jth receiver in such a system, equation (2) reduces simply to

$$\ddot{\rho}_j = \frac{A - \dot{\rho}_j^2}{\rho_j} . \tag{3}$$

If measurements of the rate of change of the Doppler frequency, $\dot{f}_j$, are made for two different times, t_o and t_1, and Doppler frequencies, f_j, are observed at regular intervals between t_o and t_1, we note that

$$\begin{aligned}
\dot{\rho}_j (t_o) &= \lambda f_j (t_o), \\
\dot{\rho}_j (t_1) &= \lambda f_j (t_1), \\
\ddot{\rho}_j (t_o) &= \lambda \dot{f}_j (t_o), \\
\ddot{\rho}_j (t_1) &= \lambda \dot{f}_j (t_1), \\
\rho_j (t_1) &= \rho_j (t_o) + \lambda \int_{t_o}^{t_1} f_j (t)\, dt,
\end{aligned} \tag{4}$$

where λ is the wavelength of the signal and, $\rho_j (t_1)$ and $\rho_j (t_o)$ are the only unknowns. Combining equations (4) with equation (3) yields

$$\rho_j (t_o) = \lambda \left[\frac{\left[f_j (t_1)\right]^2 - \left[f_j (t_o)\right]^2 + \left[\dot{f}_j (t_1)\right] \int_{t_o}^{t_1} f_j (t) dt}{\dot{f}_j (t_o) - \dot{f}_j (t_1)} - \right], \tag{5}$$

which with the last relation of equations (4) determines slant range as a function of time. These results may be used with equation (3) to establish a value for A from which an excellent approximation of the velocity of the satellite may be obtained. No additional information can be extracted when observations are limited to those from a single receiver. However, if measurements from three or more receivers overlap in time, a set of approximations to the position and velocity components may be determined by a straightforward triangulation procedure. When data from only two receivers are available, an estimate of position and velocity may still be obtained for a time which lies within the interval of observation of both receivers, if the results of the computation described by equation (5) are combined with the assumption of circular motion. For an epoch time, selected so that the satellite is near the zenith of the instrumentation site, we may safely assume that the vertical component of velocity is small and can well be approximated by zero. Using the results of the computing procedure described above, slant ranges for the epoch time may be computed for each receiver; and in the process, an estimate for the velocity of the satellite will be obtained. Combining these three results with the Doppler frequency measurements from the two receivers for epoch time, we may readily determine the remaining velocity components and all three position coordinates. In this development, no account has been taken of the difference in frequency between the transmitter in the satellite and the reference oscillator on the ground. If both are stable, a constant frequency error, or bias, will be introduced. In general, this error is so large that it must be corrected before applying the above procedure. Most methods, for determining the bias, assume symmetry about the inflection point and use this characteristic of the "S" curve to determine the inflection time as accurately as possible. Since the latter is also the time of closest approach of the satellite to the receiver, the Doppler frequency should be zero. Therefore, the bias is simply the observed frequency at the inflection time.

The second application considers a system in which the transmitter is earth-bound so that the signal travels from the Earth's surface to the satellite and back to one or more receivers on the Earth's surface. For this problem, equation (2) applies. Let us define a right-hand rectangular coordinate system as shown in Figure 9 with the origin at the transmitter and the Z-axis positive in the direction of the vertical. The y-axis is formed by the intersection of the tangent plane at the transmitter with the plane determined by the transmitter, the jth receiver, and the Earth's center. The receiver will then be at the known point $(0, y_j, z_j)$. If the variable point (x, y, z) indicates the position of the satellite, the slant ranges from the transmitter and the jth receiver are respectively given by

$$\begin{aligned} \rho_T &= \sqrt{x^2 + y^2 + z^2} \quad , \\ \rho_j &= \sqrt{x^2 + (y - y_j)^2 + (z - z_j)^2} \quad , \end{aligned} \tag{6}$$

from which it follows that

$$\begin{aligned} \dot{\rho}_T &= \frac{x\dot{x} + y\dot{y} + z\dot{z}}{\rho_T} \quad , \\ \dot{\rho}_j &= \frac{x\dot{x} + (y - y_j)\,\dot{y} + (z - z_j)\,\dot{z}}{\rho_j} \quad . \end{aligned} \tag{7}$$

In the three-beam mode of operation, the satellite will be approximately in the yz-plane at t_o, which is defined as the time halfway between the initiation and termination of tracking in the center beam. Let the satellite's position and velocity at this time be defined as (x_o, y_o, z_o) and $(\dot{x}_o, \dot{y}_o, \dot{z}_o)$, respectively. Obviously, x_o may be approximated by zero and as before, $\dot{z}_o$ may also be set equal to zero. Equations (7) then reduce to

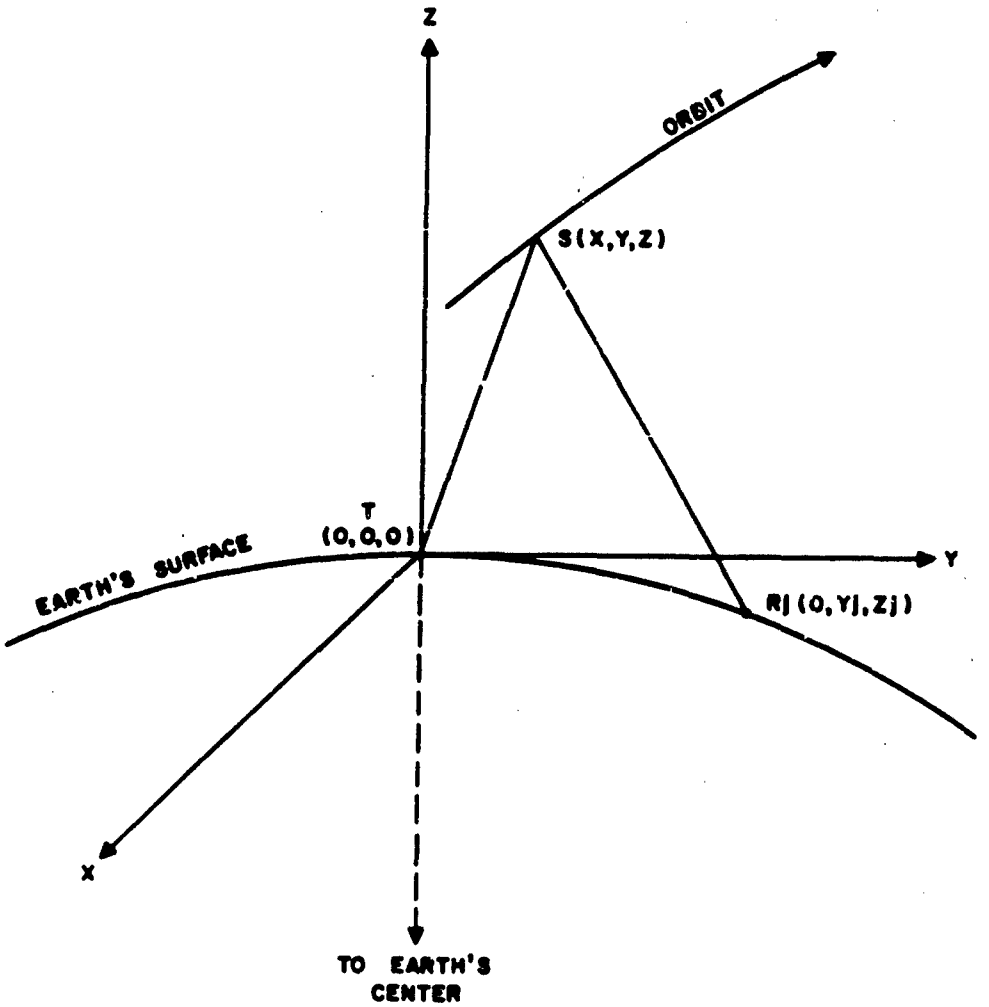

GEOMETRY FOR DETERMINING
THE INITIAL APPROXIMATIONS

FIGURE 9

$$\dot{\rho}_{To} = \frac{y_o \dot{y}_o}{\sqrt{y_o^2 + z_o^2}} \quad ,$$

$$\dot{\rho}_{jo} = \frac{(y_o - y_j)\dot{y}_o}{\sqrt{(y_o - y_j)^2 + (z_o - z_j)^2}} \quad . \tag{8}$$

Let f_{jo} and $\dot{f}_{jo}$ be the Doppler frequency and rate of change of frequency for the jth receiver at t_o. It follows that

$$f_{jo} = \frac{1}{\lambda} (\dot{\rho}_{To} + \dot{\rho}_{jo}) \quad . \tag{9}$$

From equation (2), we conclude

$$\dot{f}_{jo} = \frac{A - (\dot{\rho}_{To})^2}{\lambda \rho_{To}} + \frac{A - (\dot{\rho}_{jo})^2}{\lambda \rho_{jo}} \quad . \tag{10}$$

Expressing equations (9) and (10) in terms of the position coordinates and velocity components of the satellite at time, t_o, yields

$$f_{jo} = \frac{\dot{y}_o}{\lambda} \left[\frac{y_o}{\sqrt{y_o^2 + z_o^2}} + \frac{(y_o - y_j)}{\sqrt{(y_o - y_j)^2 + (z_o - z_j)^2}} \right] \quad , \tag{11}$$

$$\dot{f}_{jo} = \frac{A - \left[\frac{y_o \dot{y}_o}{\lambda \sqrt{y_o^2 + z_o^2}} \right]^2}{\lambda \sqrt{y_o^2 + z_o^2}} + \frac{A - \left[\frac{(y_o - y_j)\dot{y}_o}{\lambda \sqrt{(y_o - y_j)^2 + (z_o - z_j)^2}} \right]^2}{\lambda \sqrt{(y_o - y_j)^2 + (z_o - z_j)^2}} \quad . \tag{12}$$

Let us assume a specific orbital inclination. With our previous assumption of circular motion, $\dot{y}_o$ may readily be computed as a function of y_o and z_o. Then equations (11) and (12) will likewise provide f_{jo}

and $\dot{f}_{jo}$ as functions of position in the yz-plane. Thus, for a given inclination, families of curves may be computed and plotted in the yz-plane for both f_{jo} and $\dot{f}_{jo}$. Figure 10 presents such a plot, for an inclination of 80^{o}, with the transmitter and receiver separated by 434 miles and with both located 35^{o} off the equator. To attain symmetry and simplify the construction of such charts, z_j was assumed to be zero, which is a reasonable approximation for this approach to the problem. If similar charts are prepared for a number of inclinations, satisfactory initial approximations may be rather quickly and easily obtained by the following operations:

1) Assume an inclination. This, of course, is equivalent to selecting a chart. Accuracy is not essential at this stage since the estimate may be in error by 15^{o} without preventing convergence.
2) Enter the chart with the observed values of f_{jo} and $\dot{f}_{jo}$ to determine an appropriate position within the yz-plane.
3) Approximate the velocity components. These should be consistent with the assumption of circular motion, the height determined in step 2), and the assumed inclination.
4) Determine the position and velocity components in the coordinate system for the primary solution by an appropriate coordinate transformation.

In addition to the graphical method, a digital solution has been devised for equations (11) and (12). As in the previous development, we have two measurements available and desire to determine three unknowns. In this approach, one unknown is determined by establishing an upper bound and assuming a value which is a fixed distance from this bound. The distance has been selected to place the variable between its upper and lower bounds in a position which is favorable for convergence of the primary computation. In this method, we chose to start by approximating z_o. It may be observed in Figure 10 that, for larger values of $\dot{f}_{jo}$, the maximum value of z_o occurs above either the transmitter or receiver while,

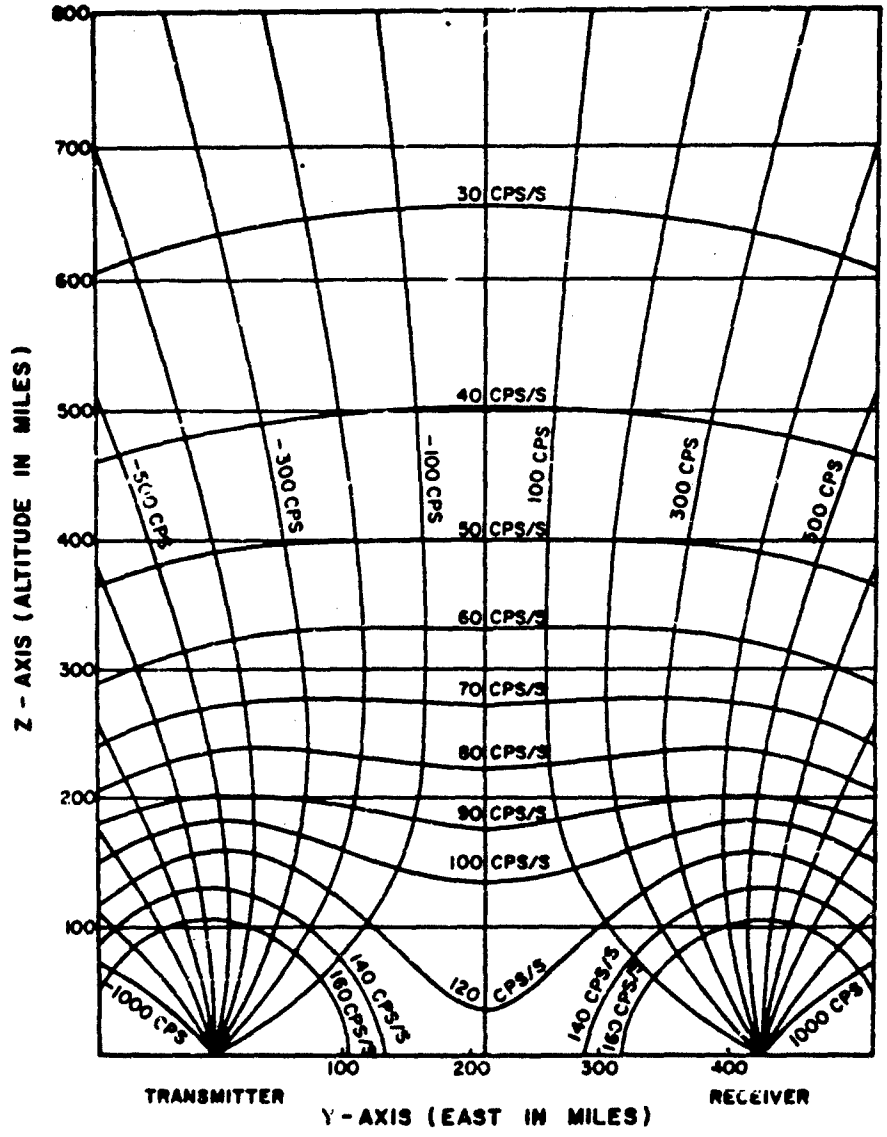

DOPLOC FREQUENCY AND RATE OF CHANGE OF FREQUENCY AS A FUNCTION OF POSITION IN THE YZ - PLANE (FOR 80° INCLINATION)

FIGURE 10

for smaller values of $\dot{f}_{jo}$, the maximum value of z_o occurs over the mid-point of the base line. The first step in the computation is to determine a maximum value for z_o. To this end, $\dot{y}_o$ is eliminated from equations (11) and (12) to yield an expression which varies only in y_o and z_o. A appears in this expression, but it is also a function of these variables. The resulting equation may be solved by numerical methods for z_o with $y_o = 0$ and then, solved a second time for z_o with $y_o = 1/2\ y_j$. The larger of these results is to be used as a value for $(z_o)_M$ which is defined to be the maximum possible value of z_o. Assuming the altitudes of all satellites to be in excess of 75 miles, we may conclude from the general characteristics of the family of curves for $\dot{f}_{jo}$ in Figure 10, that the satellite's altitude will differ from $(z_o)_M$ by no more than 100 miles. Since an error of 50 miles may be tolerated in the approximation for each coordinate, $\left[(z_o)_M - 50\right]$ is a suitable value for z_o. With the altitude thus determined, we may solve equations (11) and (12) for y_o and $\dot{y}_o$. In the process A, and hence the velocity, will be determined. With $\dot{z}_o$ assumed as zero, $\dot{x}_o$ may be readily evaluated to complete the initial approximations which consist of the position $(0, y_o, z_o)$ and the velocity $(\dot{x}_o, \dot{y}_o, 0)$. It is worth noting that there is a pair of solutions for y_o and $\dot{y}_o$. Further, the method does not determine the sign of $\dot{x}_o$. If, in addition, we accept the possibility of negative altitudes for the mathematical model, we arrive at eight possible sets of initial conditions which are approximately symmetrical with respect to the base line and its vertical bisector, It is an interesting fact that all eight, when used as input for the primary computation, lead to convergent solutions which exhibit the same type of symmetry as the approximations themselves. Of course, it is trivial to eliminate the four false solutions which place the orbit underground. Further, two additional solutions may be eliminated by noting that the order in which the satellite passes through the three antenna beams determines the sign of $\dot{x}_o$ In the two remaining possibilities, $\dot{y}_o$ is observed to have opposite signs. Since the y-axis of the DOPLOC system has been oriented from west to east, the final ambiguity may be resolved by assuming an eastward component of

velocity for the satellite - certainly a valid assumption to date. In any event, all ambiguity may be removed from the solution by the addition of one other receiver. Moreover, this would significantly improve the geometry of the system and thereby strengthen the solution.

The first method presented in this section is intended for use with a satellite which carries its own transmitter. These data are generally recorded continuously as in Figure 1a. The other two methods have been developed for a system which provides observations of the type displayed in Figure 1b where the signal source is on the Earth's surface. The plot shown in Figure 1c is also for a system with an earth-bound transmitter; and the last two methods may be applied to such data if minor modifications are made in the procedures. Indeed, with any tracking system that provides observations of satellite velocity components, equation (2) furnishes an adequate base for establishing an approximate orbit to serve as an initial solution which may be refined by more sophisticated methods.

RESULTS OF ORBITAL COMPUTATION

Numerous convergent solutions have been obtained with actual field data from a system consisting of a transmitter at Fort Sill, Oklahoma, and a single receiver at Forrest City, Arkansas. This system complex provides a base line of 434 miles. In addition, several orbits have been established from field data for satellites which carried the signal source. For the latter mode of operation, receivers were available at both Forrest City, Arkansas, and Aberdeen Proving Ground, Maryland, providing a base line of 863 miles. Results will be presented for both types of tracking.

The initial successful reduction for the Fort Sill, Forrest City system was achieved for Revolution 9937 of Sputnik III. The DOPLOC observations, as well as the results, are presented in Figure 11. Measurements were recorded for 28 seconds in the south antenna beam, 7 seconds in the center beam, and 12 seconds in the north beam, with two gaps in the data of 75 seconds. Thus, observations were recorded for a total of 47 seconds within a time interval of 3 minutes and 17 seconds. Using the graphical method described in the previous section to obtain initial approximations, convergence was achieved in three iterations on the first pass through the computing machine. It will be noted, in the comparison of DOPLOC and Space Track results, that there is good agreement in a, e, i, and Ω, particularly for the latter two. This is characteristic of the single pass solution when the eccentricity is small and the computational input is limited to Doppler frequency. Since the orbit is very close to being circular, both σ and ω are difficult for either the DOPLOC System or Space Track to determine accurately. However, as a result of the small eccentricity, $(\omega + \sigma)$ is a good approximation of the angular distance along the orbit from the equator to the position of the satellite at epoch time and as such provides a basis of comparison between the two systems. A comparison of this quantity is included in Figure 11. To summarize, when limited to single pass, single-receiver observations, the DOPLOC System provides an excellent determination of the orientation of the orbital plane, a good determination of the shape of the orbit, and a fair-to-poor determination of the orientation of the ellipse within the orbital plane.

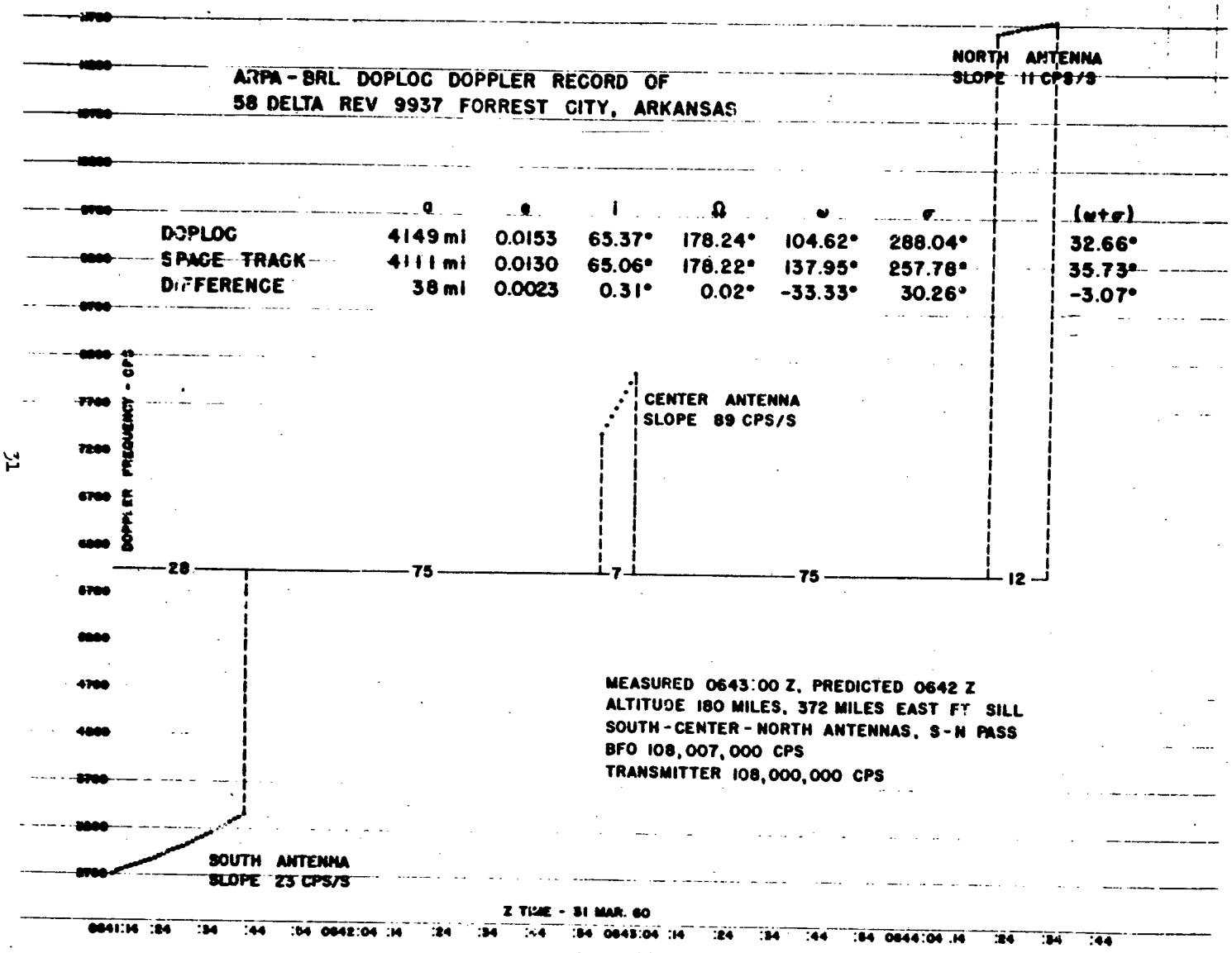

	a	e	i	Ω	ω	σ	(ω+σ)
DOPLOC	4149 mi	0.0153	65.37°	178.24°	104.62°	288.04°	32.66°
SPACE TRACK	4111 mi	0.0130	65.06°	178.22°	137.95°	257.78°	35.73°
DIFFERENCE	38 mi	0.0023	0.31°	0.02°	-33.33°	30.26°	-3.07°

FIGURE 11

Although σ and ω have been accurately determined on occasion, the interim DOPLOC system with its limitations fails to provide consistently good results for these two quantities. Therefore, only a, e, i, and Ω will be considered in presenting the remaining DOPLOC reductions. The observations recorded for the Fort Sill, Forrest City complex are plotted in Figure 12 for six revolutions of Discoverer XI including 172, the last known revolution of this satellite. The DOPLOC determined position for this pass indicated an altitude of 82 miles as the satellite crossed the base line 55 miles west of Forrest City. A comparison of the Space Track results with the DOPLOC reductions for these observations is presented in Figures 13 through 16. In addition, DOPLOC reductions have been included for three revolutions in which the receivers at Forrest City and Aberdeen Proving Ground tracked the air-borne transmitter in the satellite. In Figures 17 through 20 a similar comparison is presented for six separate passes of Transit 1B. In these, all observations consist of data obtained by receivers at Forrest City and Aberdeen Proving Ground while tracking the on-board transmitter.

Finally, in Figure 21, results are tabulated for a reduction based on only seven frequency observations. These have been extracted from the complete set of observations previously presented for Sputnik III. They were selected to serve as a crude example of the type of reduction required for the proposed DOPLOC scanning-beam system. The example shows that the method is quite feasible for use with periodic, discrete measurements of frequency. Of course, the proposed system would normally yield several more observations than were available in the example.

It is noteworthy that numerous solutions have been obtained with field data from a single receiver during a single pass of a satellite. Further, these measurements have been confined to three short periods of observation within a two to three minute interval. Additional receivers spread over greater distances would, of course, considerably enhance the accuracy of the results. For example, a system with two receivers and a

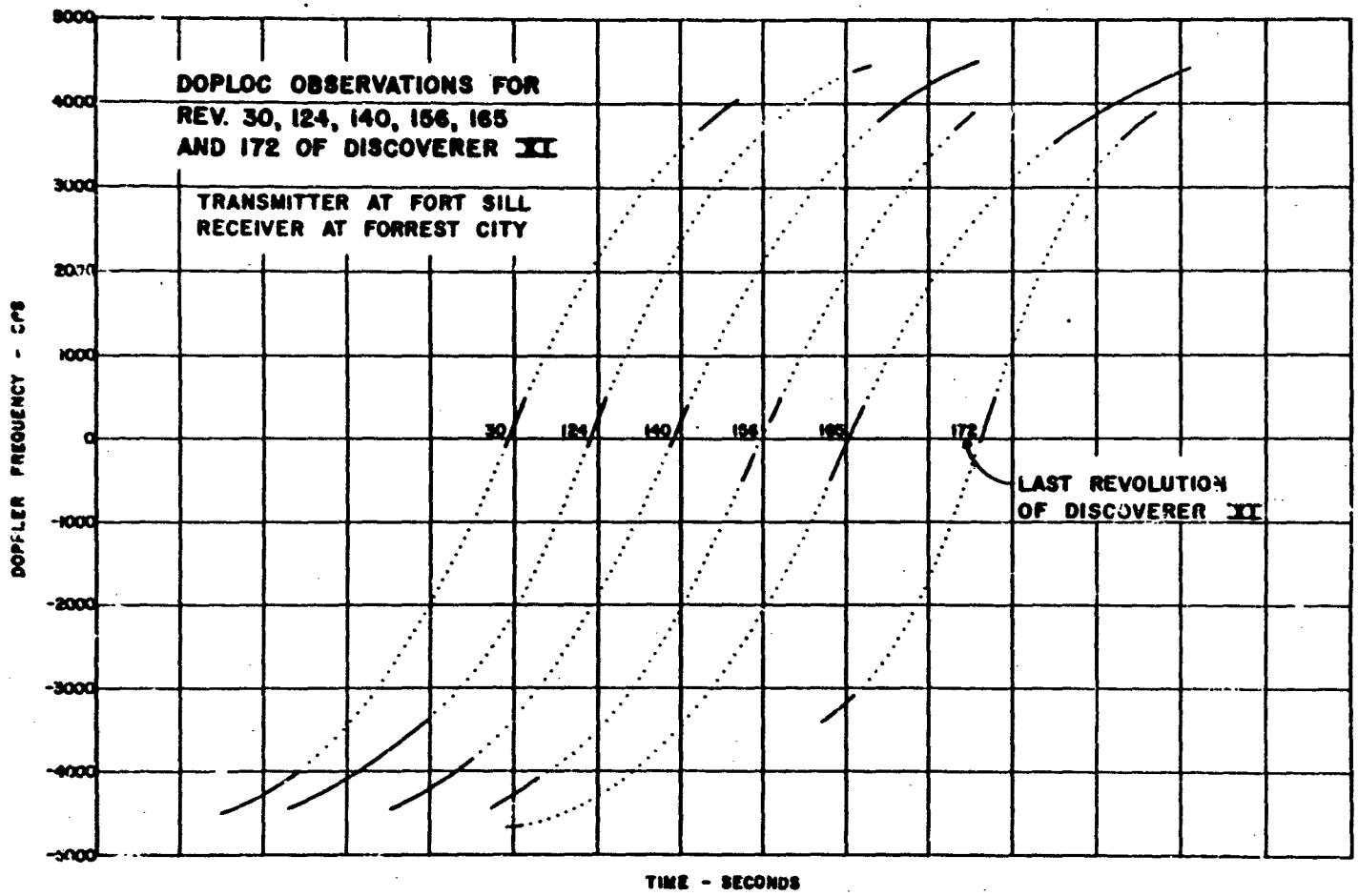
DOPLOC OBSERVATIONS FOR
REV. 30, 124, 140, 156, 165
AND 172 OF DISCOVERER XI
TRANSMITTER AT FORT SILL
RECEIVER AT FORREST CITY
30
124
140
156
165
172
LAST REVOLUTION
OF DISCOVERER XI
DOPPLER FREQUENCY - CPS
TIME - SECONDS

FIGURE 12

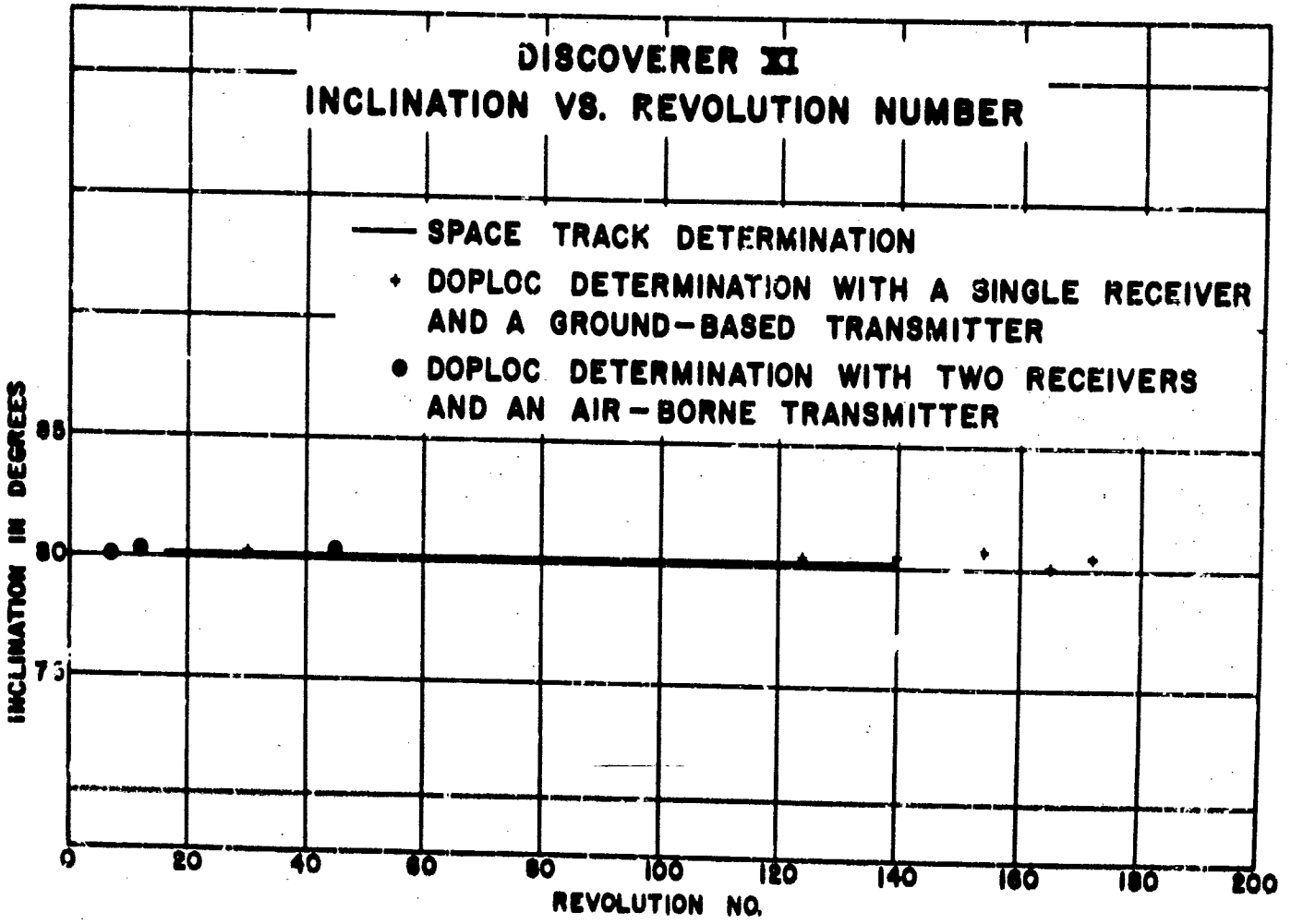
DISCOVERER XI
INCLINATION VS. REVOLUTION NUMBER
SPACE TRACK DETERMINATION
DOPLOC DETERMINATION WITH A SINGLE RECEIVER AND A GROUND-BASED TRANSMITTER
DOPLOC DETERMINATION WITH TWO RECEIVERS AND AN AIR-BORNE TRANSMITTER
INCLINATION IN DEGREES
85
80
75
0
20
40
60
80
100
120
140
160
180
200
REVOLUTION NO.

FIGURE 13

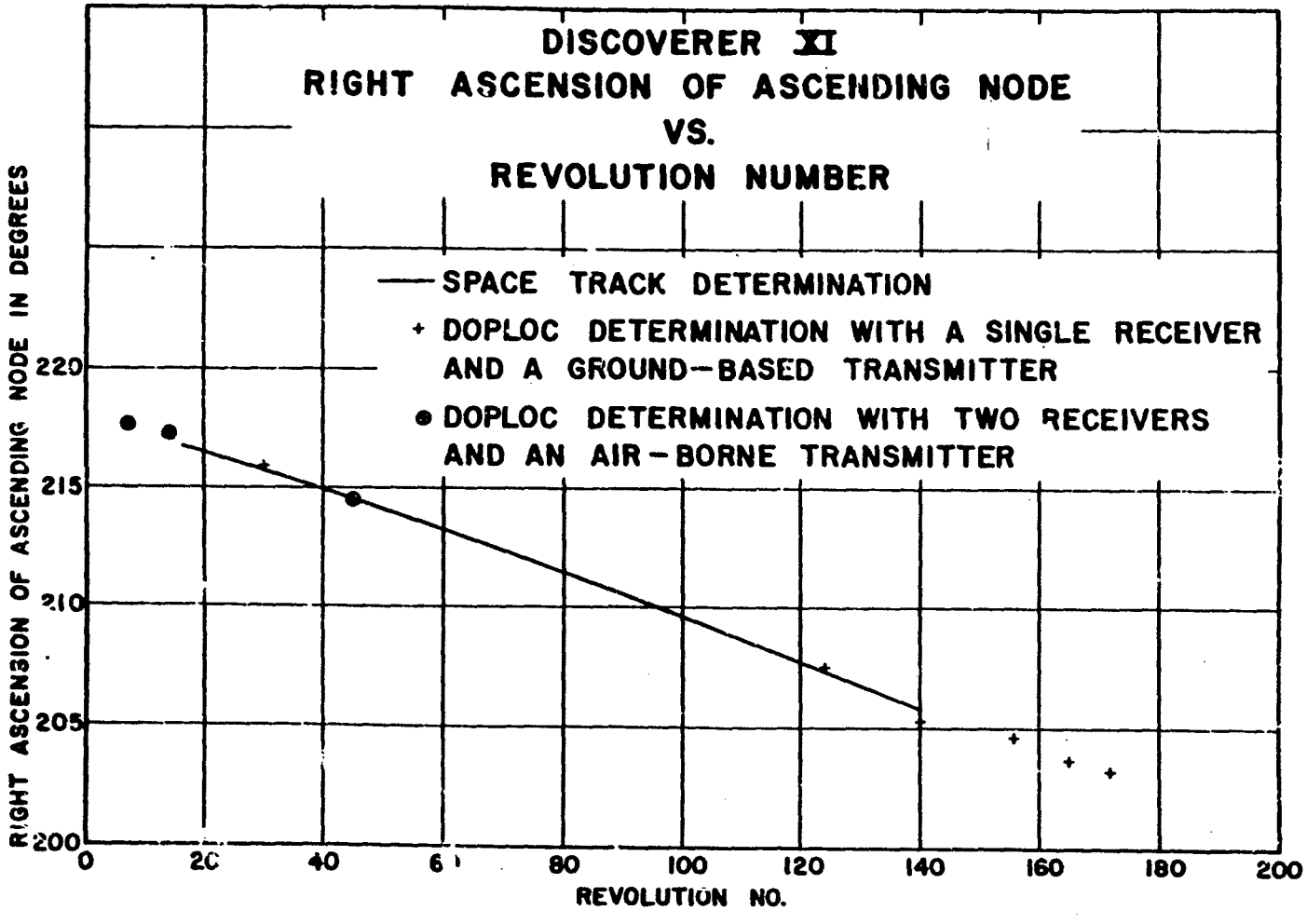
DISCOVERER XI
RIGHT ASCENSION OF ASCENDING NODE
VS.
REVOLUTION NUMBER
SPACE TRACK DETERMINATION
DOPLOC DETERMINATION WITH A SINGLE RECEIVER AND A GROUND-BASED TRANSMITTER
DOPLOC DETERMINATION WITH TWO RECEIVERS AND AN AIR-BORNE TRANSMITTER
RIGHT ASCENSION OF ASCENDING NODE IN DEGREES
220
215
210
205
200
0
20
40
60
80
100
120
140
160
180
200
REVOLUTION NO.

FIGURE 14

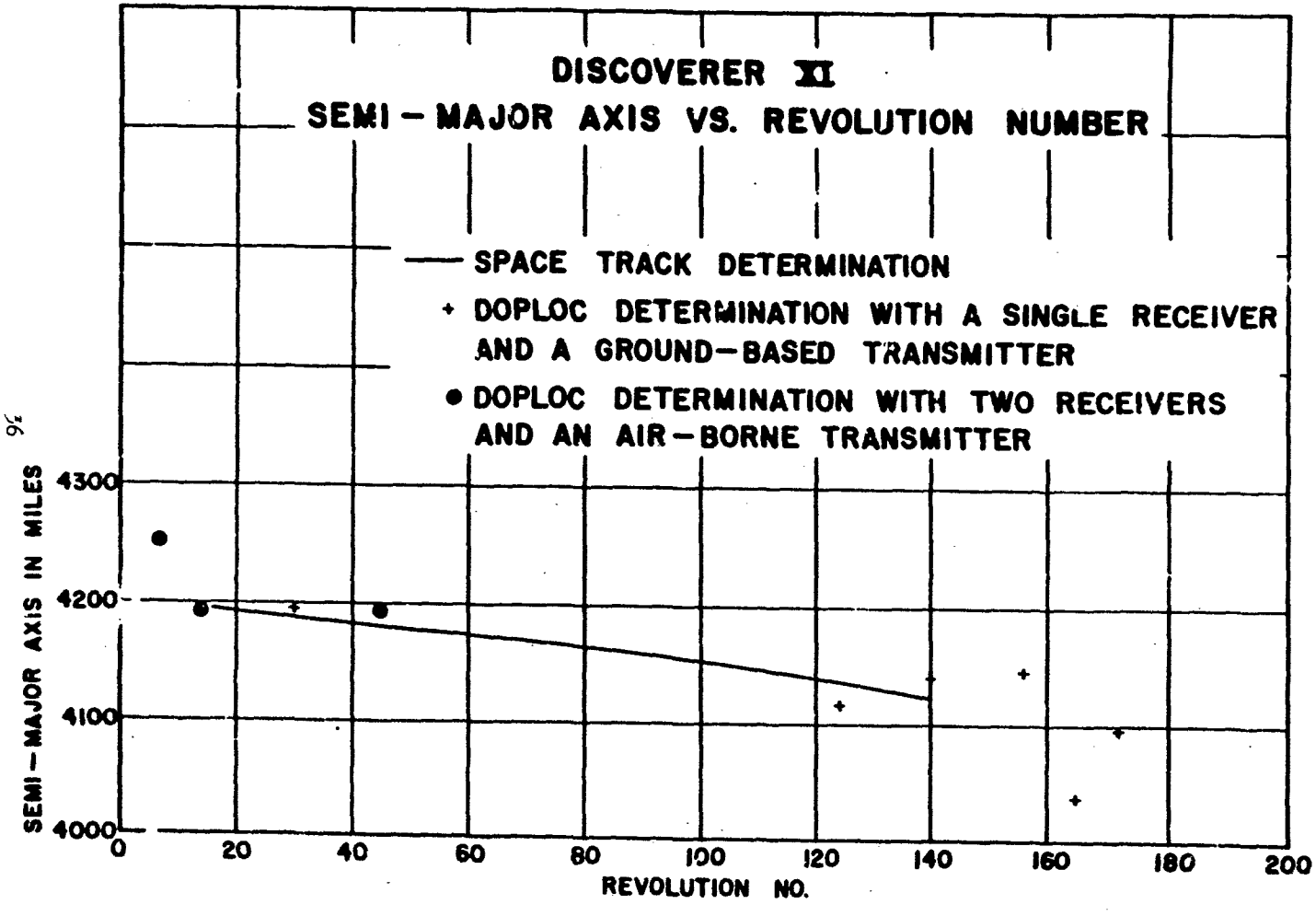
DISCOVERER XI
SEMI-MAJOR AXIS VS. REVOLUTION NUMBER
SPACE TRACK DETERMINATION
DOPLOC DETERMINATION WITH A SINGLE RECEIVER AND A GROUND-BASED TRANSMITTER
DOPLOC DETERMINATION WITH TWO RECEIVERS AND AN AIR-BORNE TRANSMITTER
SEMI-MAJOR AXIS IN MILES
4300
4200
4100
4000
0
20
40
60
80
100
120
140
160
180
200
REVOLUTION NO.

FIGURE 15

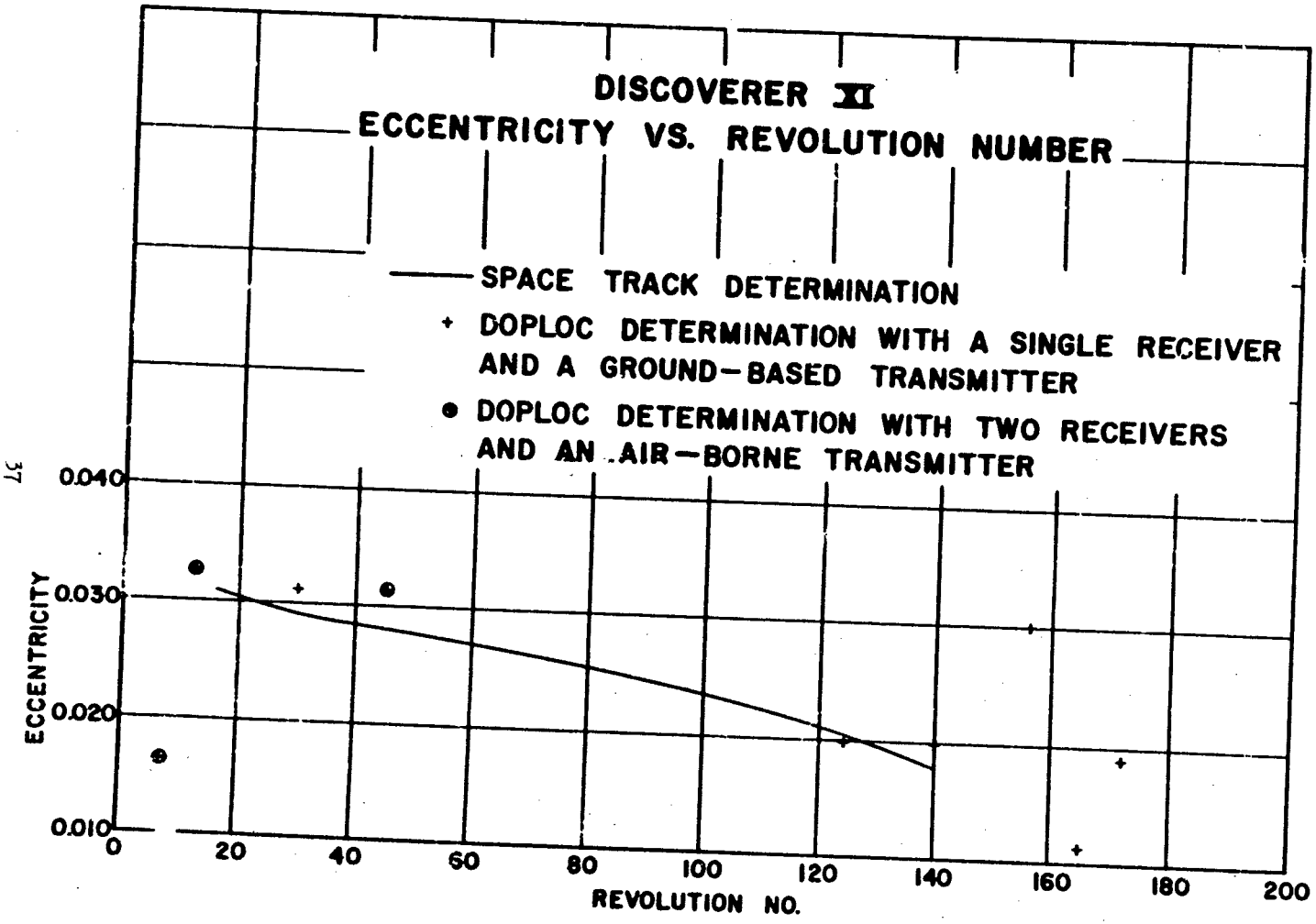
DISCOVERER XI
ECCENTRICITY VS. REVOLUTION NUMBER
SPACE TRACK DETERMINATION
DOPLOC DETERMINATION WITH A SINGLE RECEIVER AND A GROUND-BASED TRANSMITTER
DOPLOC DETERMINATION WITH TWO RECEIVERS AND AN AIR-BORNE TRANSMITTER
ECCENTRICITY
0.040
0.030
0.020
0.010
0
20
40
60
80
100
120
140
160
180
200
REVOLUTION NO.

FIGURE 16

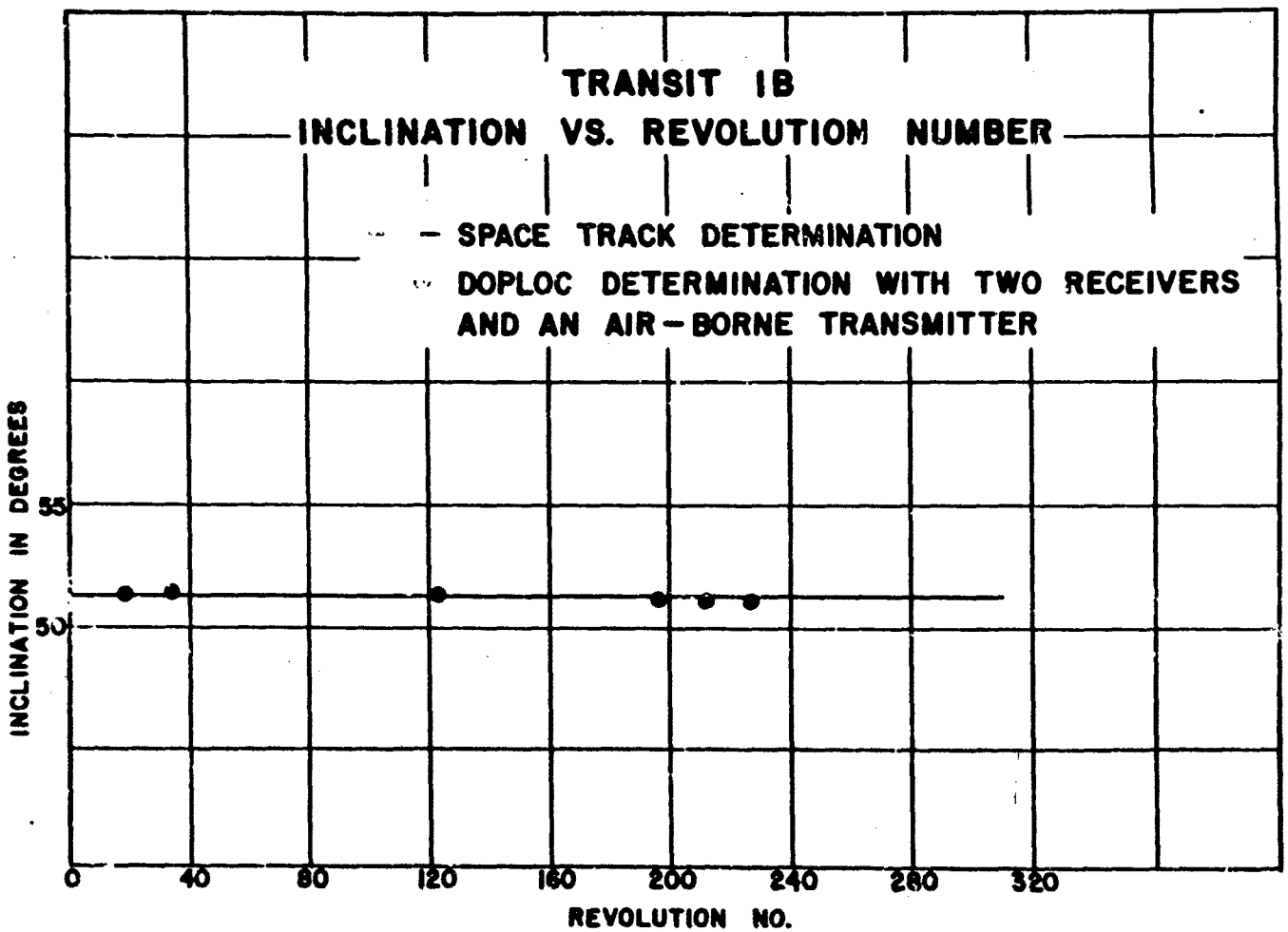
TRANSIT 1B
INCLINATION VS. REVOLUTION NUMBER
– SPACE TRACK DETERMINATION
DOPLOC DETERMINATION WITH TWO RECEIVERS AND AN AIR-BORNE TRANSMITTER
INCLINATION IN DEGREES
55
50
0
40
80
120
160
200
240
280
320
REVOLUTION NO.

FIGURE 17

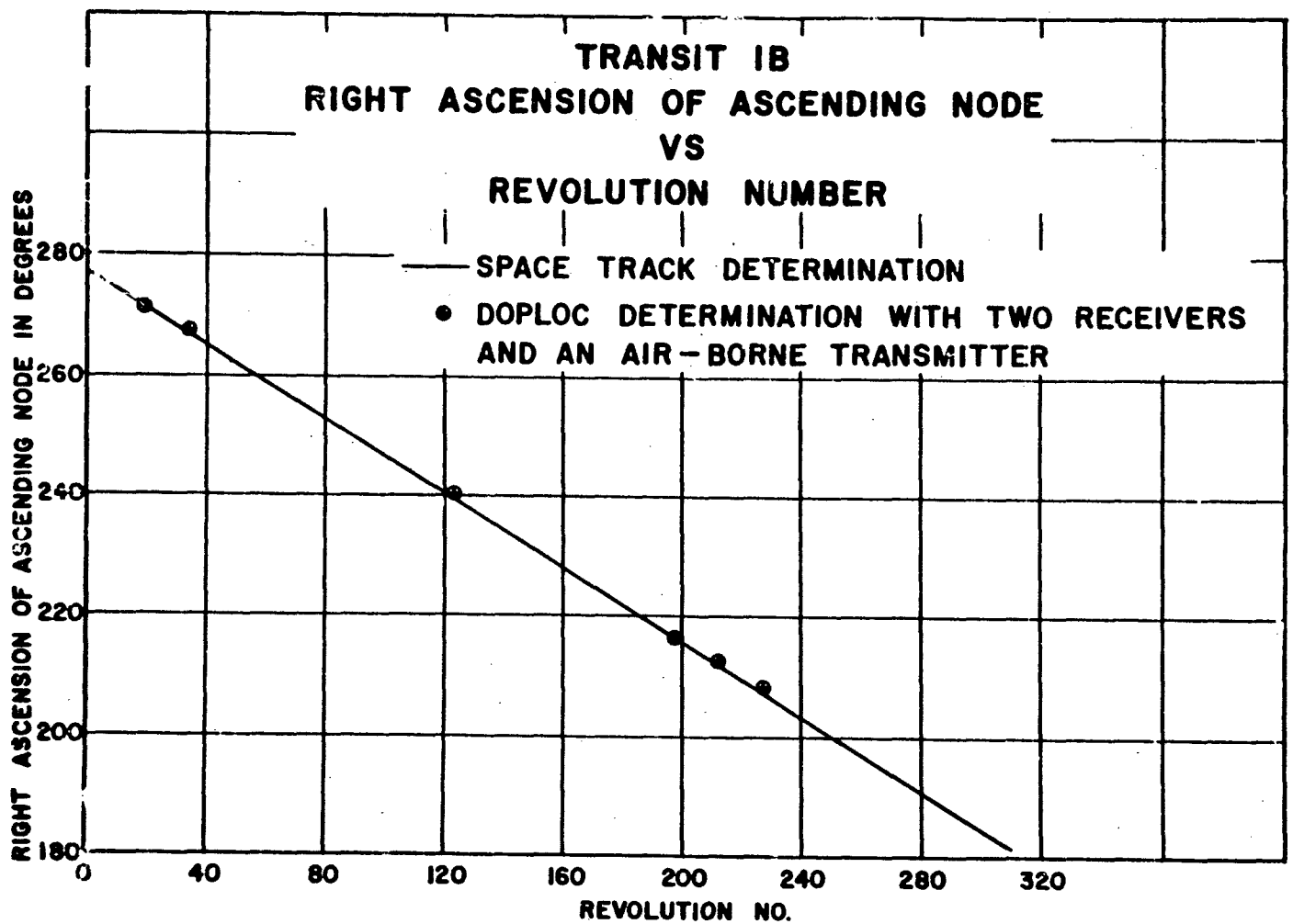
TRANSIT 1B
RIGHT ASCENSION OF ASCENDING NODE
VS
REVOLUTION NUMBER
SPACE TRACK DETERMINATION
DOPLOC DETERMINATION WITH TWO RECEIVERS AND AN AIR-BORNE TRANSMITTER
RIGHT ASCENSION OF ASCENDING NODE IN DEGREES
280
260
240
220
200
180
0
40
80
120
160
200
240
280
320
REVOLUTION NO.

FIGURE 18

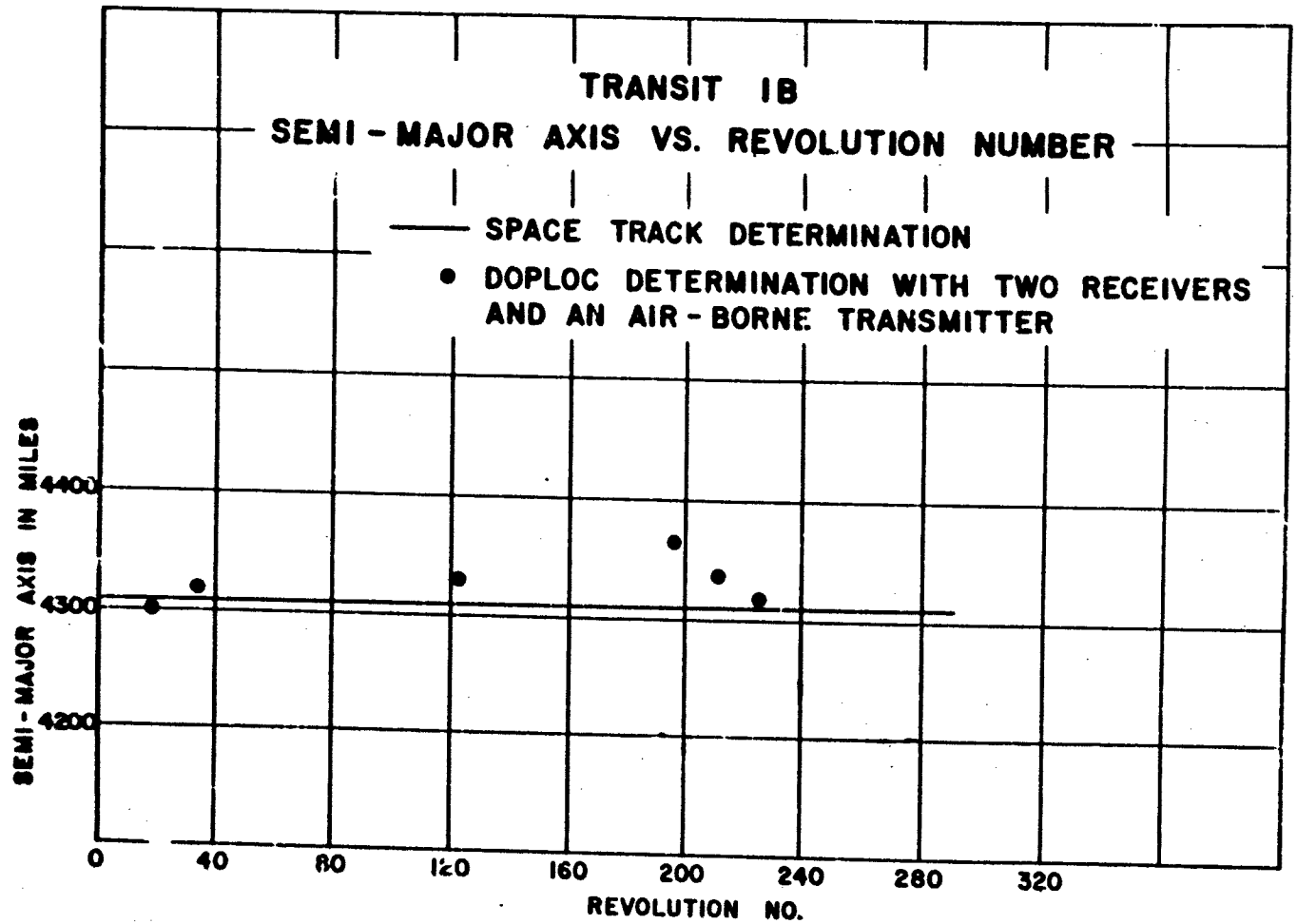
TRANSIT 1B
SEMI-MAJOR AXIS VS. REVOLUTION NUMBER
SPACE TRACK DETERMINATION
DOPLOC DETERMINATION WITH TWO RECEIVERS AND AN AIR-BORNE TRANSMITTER
SEMI-MAJOR AXIS IN MILES
4400
4300
4200
0
40
80
120
160
200
240
280
320
REVOLUTION NO.

FIGURE 19

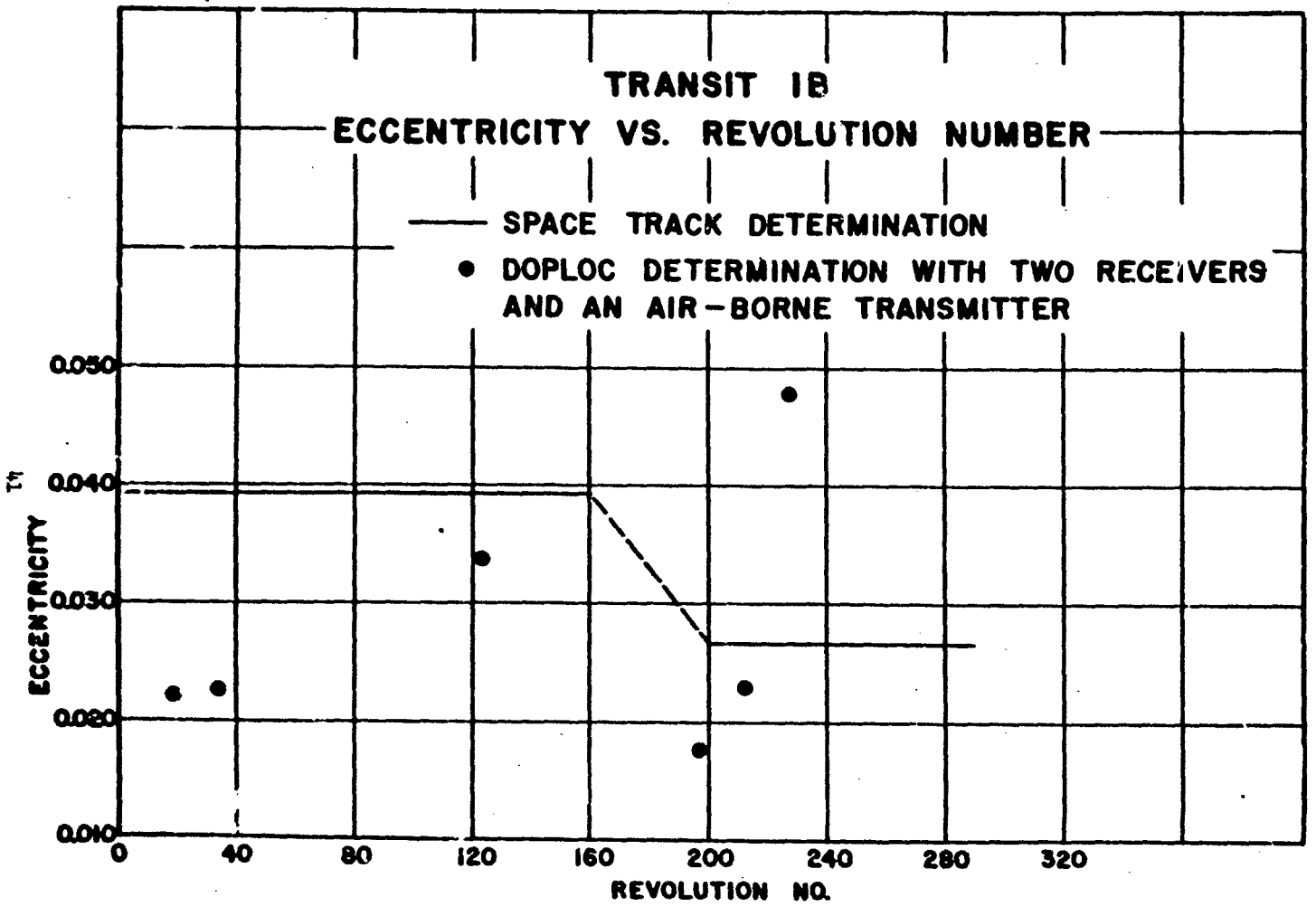
TRANSIT 1B
ECCENTRICITY VS. REVOLUTION NUMBER
SPACE TRACK DETERMINATION
DOPLOC DETERMINATION WITH TWO RECEIVERS AND AN AIR-BORNE TRANSMITTER
ECCENTRICITY
0.050
0.040
0.030
0.020
0.010
0
40
80
120
160
200
240
280
320
REVOLUTION NO.

FIGURE 20

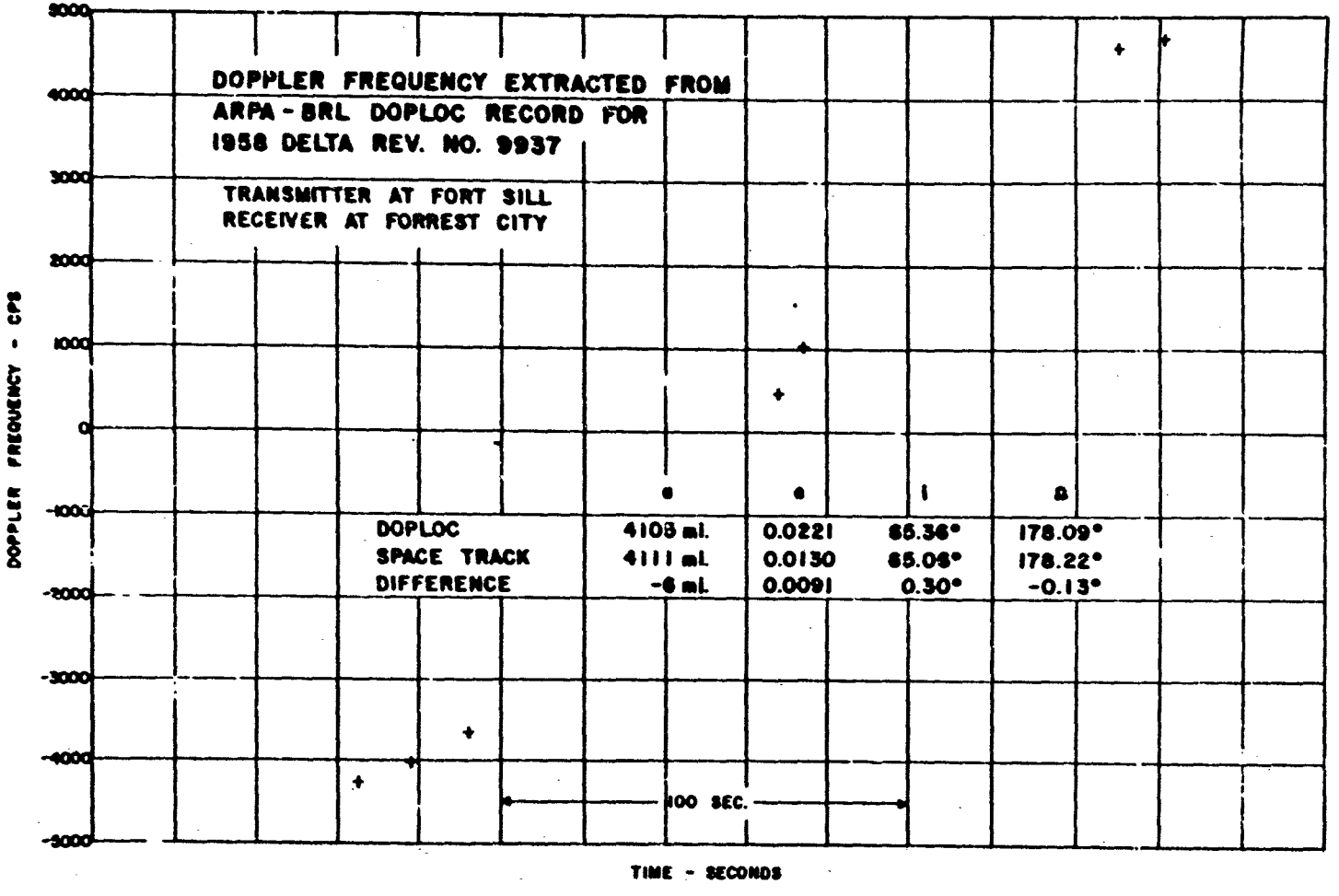
DOPPLER FREQUENCY EXTRACTED FROM
ARPA - BRL DOPLOC RECORD FOR
1958 DELTA REV. NO. 9937
TRANSMITTER AT FORT SILL
RECEIVER AT FORREST CITY
DOPLOC 4108 mi. 0.0221 85.36° 178.09°
SPACE TRACK 4111 mi. 0.0130 85.08° 178.22°
DIFFERENCE -6 mi. 0.0091 0.30° -0.13°
100 SEC.
DOPPLER FREQUENCY - CPS
TIME - SECONDS

FIGURE 21

ground transmitter would reduce error propagation in the computations to approximately a tenth of that to be expected for a system with a single receiver. Removing the restriction of single pass determination would further enhance the accuracy of the results.

Computing times have been found to be quite reasonable. Convergent solutions have required 20 to 40 minutes on the Ballistic Research Laboratories' ORDVAC which requires the coding to include floating decimal sub-routines. More modern machines, such as the BRLESC, now under construction at the Ballistic Research Laboratories, will perform the same computation in 2 to 4 minutes. Hence, it is realistic to claim that the system potentially has the capability of orbit determination within five minutes of the observation time. In conclusion, the method is general and, therefore, need be confined to neither Doppler frequencies nor Keplerian orbits. In particular, if the limitation of Keplerian motion may be retained, only minor modification is required to use the method with all other types of satellite observations.

IONOSPHERIC MEASUREMENTS

One of the methods used for studying the ionosphere is derived from the measurement of its effect on radio waves propagated through it. One effect observed is the increase in propagation phase velocity above that occurring in free space (i.e. the wavelength is longer in the medium than in free space). At the frequencies used, 30 to 300 mc., the index of refraction can be expressed as

$$\mu \doteq 1 - \frac{40.25\, N_e}{f_o^2}, \tag{13}$$

where N_e is the electron density in electrons per cubic meter and f_o is the transmitted frequency. Thus, the index of refraction is less than unity in an ionized medium and the amount by which the index of refraction is changed is inversely proportional to the square of the frequency.

Use is made of the dependence of the refractive index on frequency to determine ionosphere electron content. Data with which to make the electron content computation are obtained by measuring the Doppler frequency shift on two harmonically related signal frequencies transmitted from a satellite. The Doppler frequency, superimposed upon the lower of the two frequencies, is multiplied by the ratio of the two signal frequencies employed; and then the result is subtracted from the Doppler observations of the higher frequency signal to yield dispersive Doppler data. The dispersive Doppler frequency is proportional to the time rate of change of the total electron content along the propagation path,

$$f_{DD} \propto \frac{d}{dt} \int_o^r N_e dr, \tag{14}$$

where $\int_o^r N_e dr$ is the total electron content along the propagation path, r. Thus a measure of the change in electron content, over a time interval of interest, is obtained by integration of the dispersive Doppler frequency, which is simply a cycle count over the specified interval.

Instrumentation has been developed for measuring and recording dispersive Doppler frequency. Satellites carrying radio transmitters whose frequencies are harmonically related serve as signal sources. In order to receive signals from satellites at great distances and provide output data of high quality it is necessary to use extremely sensitive receiving systems. Narrow bandwidth, phase-locked, tracking filters are used to provide essentially noise-free Doppler frequency data. Two channels are used to receive the two harmonically related signals. The multiplication of the Doppler frequency on the lower frequency signal takes place at the output of the tracking filter so as not to degrade the signal-to-noise ratio. Frequency multiplication prior to the final narrow-bandwidth filter would seriously degrade the signal-to-noise ratio of the Doppler signal. A special broadband frequency multiplier (ref. 4) has been developed for multiplying audio frequencies. The technique developed is unique in that it achieves multiplication of an audio frequency Doppler signal, which varies many octaves, but maintains a sinusoidal output waveform. The multiplication factor can be any product of two's and three's (i.e. 2, 3, 4, 6, 8, 9, ---.). This frequency multiplier is basically a combination of an aperiodic frequency doubler, push-push, circuit and a bridge configuration tripler circuit. Auxiliary circuits with functions of automatic gain control, clipping, differentiation and phase-locked tracking filtering make possible a sinusoidal output waveform.

Figure 22 shows a block diagram of a receiving system for ionospheric measurements using the broadband frequency multiplier (ref. 5). Dispersive Doppler, Faraday rotation and satellite rotation effects on the signal can be separated automatically and directly recorded as shown in Figure 23. This is a portion of a record from an upper atmosphere sounding rocket flight in which a two frequency transmitter was carried.

Dispersive Doppler data recorded in a form similar to that shown in Figure 23 can be counted to an accuracy of $\pm$ 0.1 cycle. The total electron content can be expressed in terms of dispersive Doppler cycles as

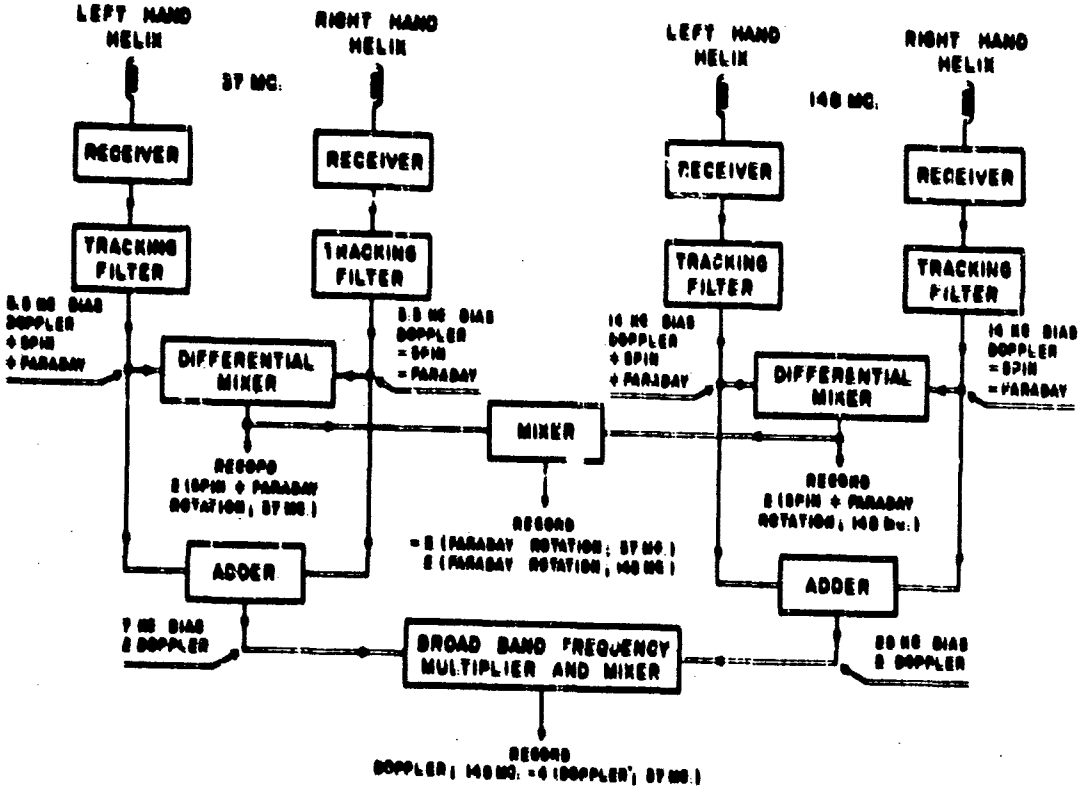

FIGURE - IONOSPHERE PROBE - GROUND STATION BLOCK DIAGRAM

FIGURE

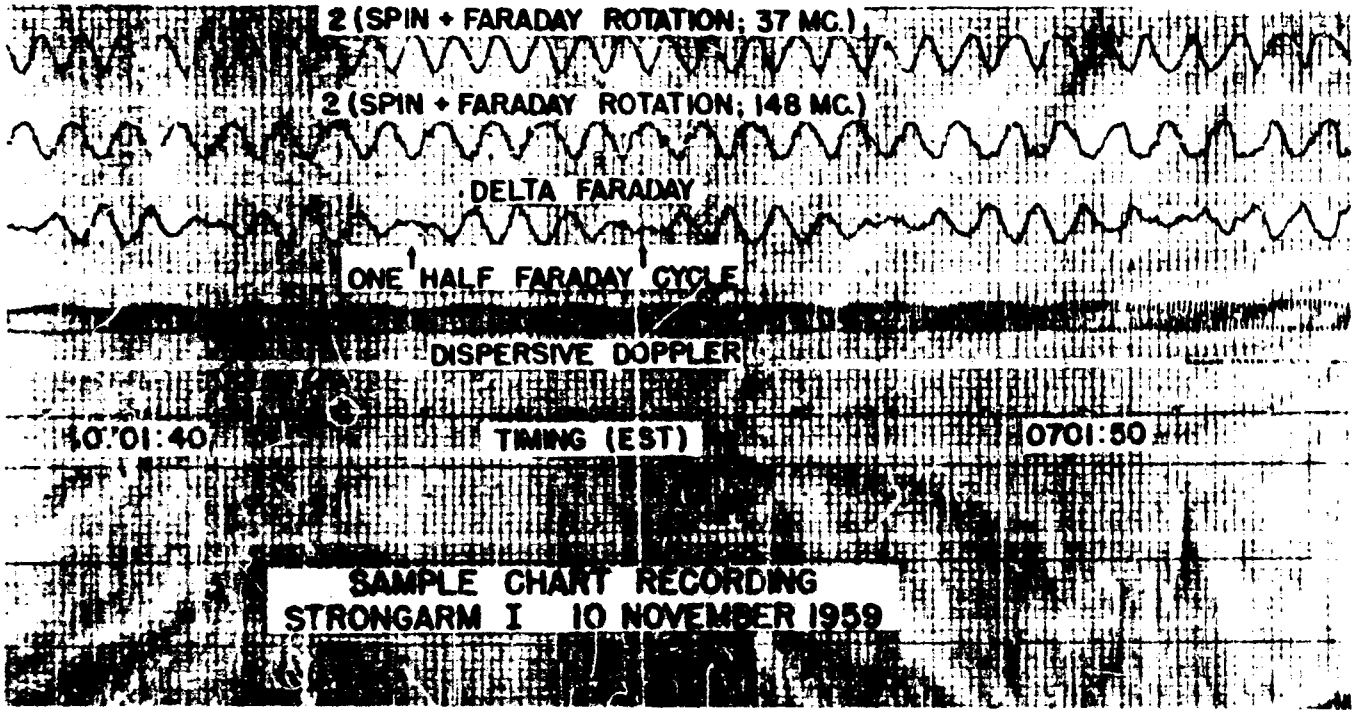
2 (SPIN + FARADAY ROTATION; 37 MC.)
2 (SPIN + FARADAY ROTATION; 148 MC.)
DELTA FARADAY
ONE HALF FARADAY CYCLE
DISPERSIVE DOPPLER
0701:40
TIMING (EST)
0701:50
SAMPLE CHART RECORDING
STRONGARM I 10 NOVEMBER 1959

FIGURE 23

$$N_e dr = (\phi_2 - K\phi_1) \frac{F_2}{(K^2 - 1)\ 13.4 \times 10^{-8}} , \qquad (15)$$

where $(\phi_2 - K\phi_1)$ is the integrated dispersive Doppler frequency, F_1 is the lower transmission frequency, F_2 is the higher, K is the ratio F_2/F_1. Consider the Transit satellite (1960 Eta), where F_1 = 54 mc and F_2 = 324 mc. The incremental change in total electron content for each dispersive Doppler cycle is

$$N_e dr = \frac{3.24 \times 10^8}{\left[\left(\frac{324}{54}\right)^2 - 1\right] \times 13.4 \times 10^{-8}} = 6.9 \times 10^{13} \ \frac{\text{electrons}}{\text{square meter}} . \qquad (16)$$

Therefore, the counting accuracy of $\pm$ 0.1 cycle represents a measuring sensitivity to the change in ionosphere electron content of 6.9×10^{12} electrons/square meter. This sensitivity is high enough to detect small irregularities in the ionosphere. A plot of dispersive Doppler data and integrated dispersive Doppler frequency is shown in Figure 24 for a pass of the Transit satellite (1960 Eta) on 17 November 1960. Irregular horizontal gradients in the ionosphere are clearly shown by the variations in the dispersive Doppler frequency that are evident during the second half of the satellite pass. This curve normally has a relatively smooth "S" shape under undisturbed geomagnetic conditions. It is of considerable interest to note that this record was made following the period of an extremely severe geomagnetic disturbance. Severely disturbed radio conditions existed from November 12 through 18. One of the most active solar regions observed in recent years was reported by the North Atlantic Radio Warning Service of the National Bureau of Standards. The A-index (a measure of geomagnetic activity) on November 13 was 280, the highest recorded in this solar cycle. An A-index of 25 is considered a disturbed condition, therefore 280 represents an extremely disturbed condition. An unusually high magnetic field intensity was recorded at the Ballistic Research Laboratories magnetometer station on November 12 and 13 which is shown in

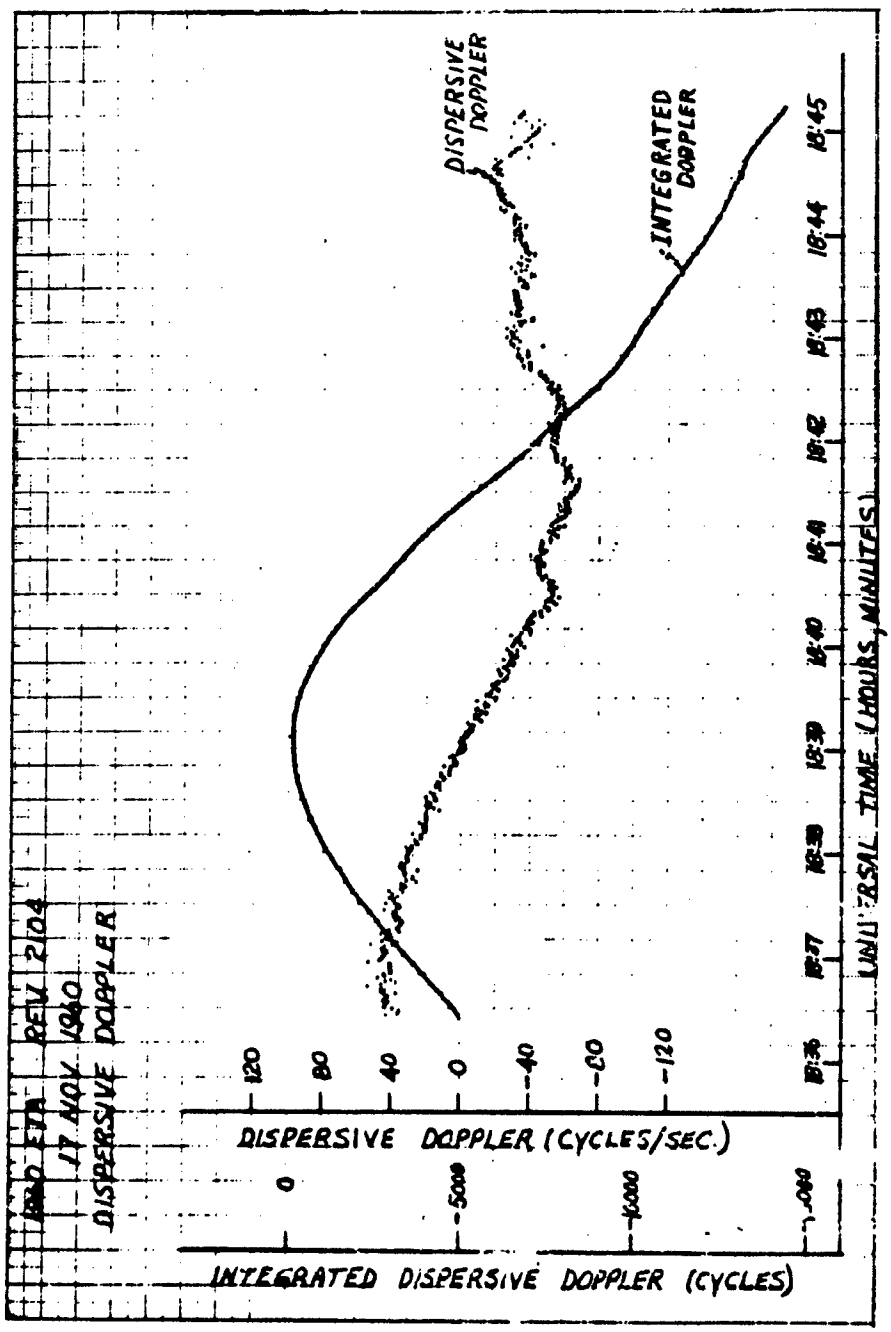
DISPERSIVE DOPPLER
INTEGRATED DOPPLER
DISPERSIVE DOPPLER (CYCLES/SEC.)
INTEGRATED DISPERSIVE DOPPLER (CYCLES)
UNIVERSAL TIME (HOURS, MINUTES)
DISPERSIVE DOPPLER
17 NOV 1980
REV 2104

FIGURE 24

Figure 25. Thus the qualitative agreement between the irregularly shaped dispersive Doppler curve in Figure 24 and the disturbed ionosphere is well established.

The Faraday rotation effect can also be used to determine total ionosphere content. Techniques have been developed for separating Faraday rotation effects from satellite rotation effects by the use of opposing circularly polarized antennas and a sequence of electronic mixers as shown in Figure 22. When the satellite spins very slowly, a simpler method of determining Faraday rotation cycles by counting received signal amplitude nulls can be used. A linearly polarized receiving antenna is used in this case. A plot of ionospheric electron content is shown in Figure 26, obtained by using received signal amplitude null data from a pass of the Transit satellite (1960 Eta). The computation methods of Bowhill (ref. 6) and Garriott (ref. 7) were used in the earliest studies. A complete ray tracing program based on that of Little and Lawrence (ref. 8) is in preparation to provide more accuracy and to eliminate several assumptions and restrictions of the early methods.

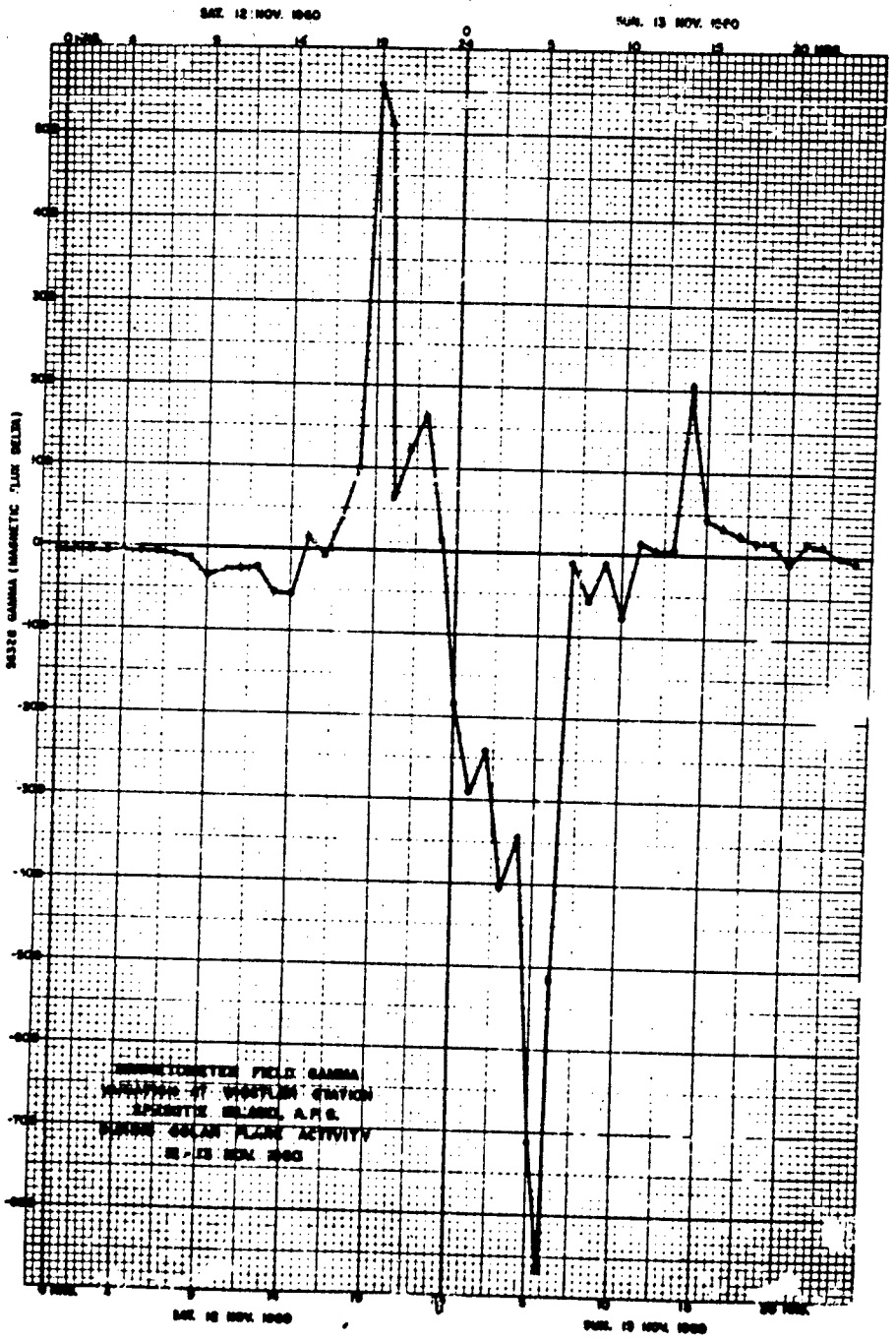

FIGURE 25

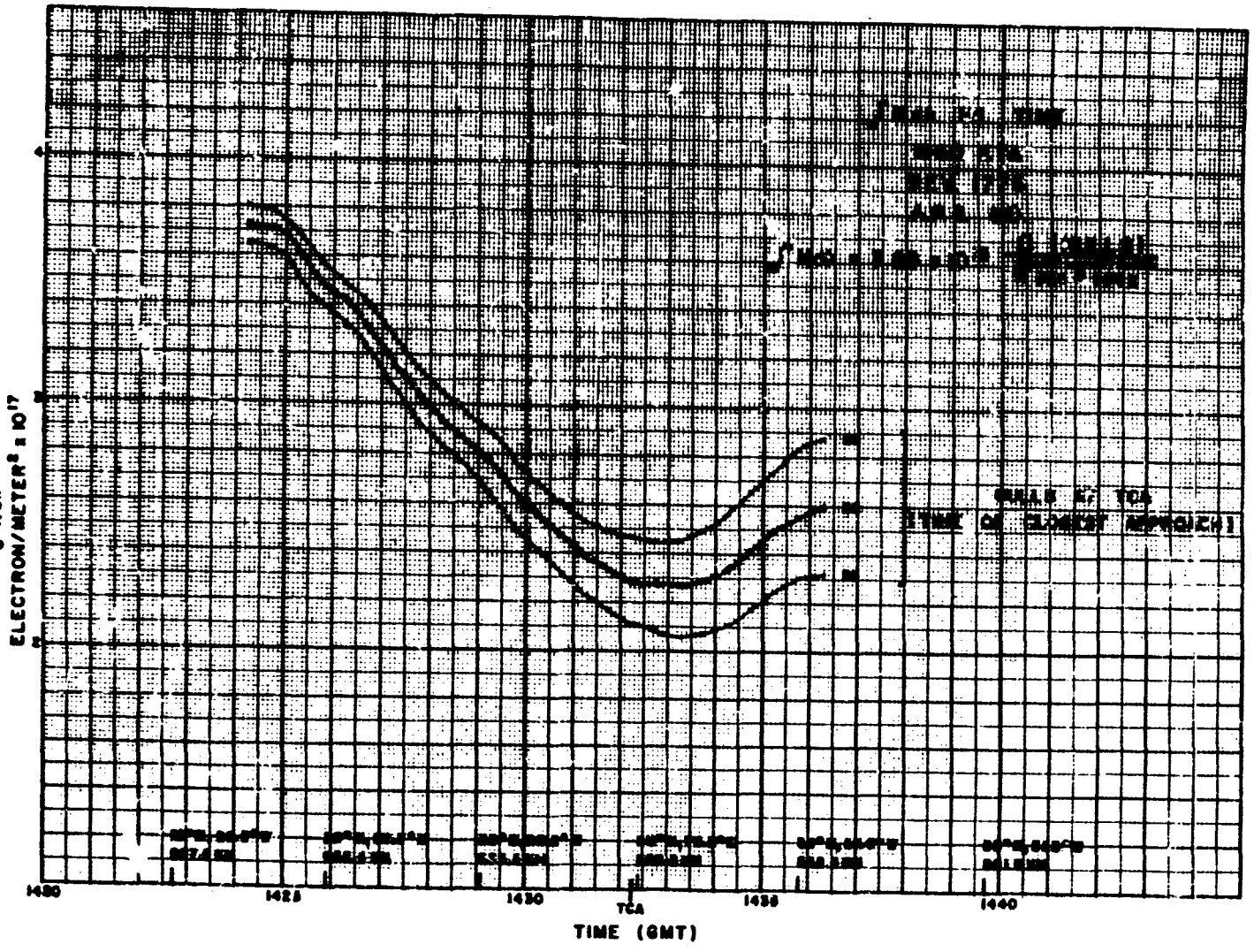

FIGURE 26

CONCLUSIONS

The information on the ionosphere, obtained by the methods described, makes it possible to correct refraction errors and obtain more accurate orbital parameters from Doppler data. An interesting example of the ionospheric effect on orbital accuracy was observed in the computation of the orbital parameters shown in Figures 17, 18, 19, and 20. The computation was first attempted using the complete "S" curve including the relatively constant frequency limbs. The limbs represent data obtained during the emergence of the satellite from the horizon and recession into the horizon. The orbit obtained was appreciably different from that published by Space Track. Another computation was made using only the center portion of the "S" curve, while disregarding the limbs. The solution was greatly improved and the results agreed very well with Space Track data. This points out the large refractive effect the ionosphere introduces at low elevation angles of transmission. Fortunately, an orbital solution can be computed from Doppler data obtained at quite high elevation angles, thereby minimizing the refractive error.

A program has been initiated to combine Doppler frequency observations with electron content data in an iterative computing process to increase the accuracy of the orbital determination. The computation will be initiated by determining an orbit from the uncorrected Doppler observations. The electron content data and this approximate orbit will be combined to compute corrections for the original Doppler frequency measurements. Using the latter, the process will be iterated until the refractive error has been minimized in the Doppler data and hence, in the computed orbital parameters as well.

R. B. Patton, Jr.
R. B. PATTON, JR.

Victor W. Richard
V. W. RICHARD

REFERENCES

1. Richard, Victor W. DOPLOC Tracking Filter, BRL Memorandum Report 1173, October 1958, Ballistic Research Laboratories, Aberdeen Proving Ground, Maryland.

2. Dean, William A. Precision Frequency Measurement of Noisy Doppler Signal, BRL Memorandum Report 1110, June 1960, Ballistic Research Laboratories, Aberdeen Proving Ground, Maryland.

3. Patton, Robison B., Jr. Orbit Determination from Single Pass Doppler Observations, IRE Transactions on Military Electronics, Vol MIL-4, Numbers 2 & 3, pp 339-344, April - July, 1960.

4. Patterson, Kenneth H. A Broadband Frequency Multiplier and Mixer for Dispersive Doppler Measurements, BRL Memorandum Report 1343, March 1961, Ballistic Research Laboratories, Aberdeen Proving Ground, Maryland

5. Cruickshank, William J. Instrumentation Used for Ionosphere Electron Density Measurements, BRL Technical Note 1317, May 1960, Ballistic Research Laboratories, Aberdeen Proving Ground, Maryland.

6. Bowhill, S. A. The Faraday Rotation Rate of a Satellite Radio Signal, Journal of Atmospheric and Terrestrial Physics, 13 (1 and 2), 175, 1958.

7. Garriott, O. K. The Determination of Ionospheric Electron Content and Distribution from Satellite Observations, Theory and Results, Journal of Geophysical Research 65, 4, April 1960.

8. Little, C. G. and Lawrence, R. S. The Use of Polarization Fading of Satellite Signals to Study Electron Content and Irregularities in the Ionosphere, National Bureau of Standards Journal of Research, V64D, No. 4, July - August 1960.

DISTRIBUTION LIST

No. of Copies	Organization
1	Chief of Ordnance ATTN: ORDTB - Bal Sec Department of the Army Washington 25, D.C.
1	Commanding Officer Diamond Ordnance Fuze Laboratories ATTN: Technical Information Office, Branch 041 Washington 25, D.C.
10	Commander Armed Services Technical Information Agency ATTN: TIPCR Arlington Hall Station Arlington 12, Virginia
10	Commander British Army Staff British Defence Staff (W) ATTN: Reports Officer 3100 Massachusetts Avenue, N.W. Washington 8, D.C.
4	Defence Research Member Canadian Joint Staff 2450 Massachusetts Avenue, N.W. Washington 8, D.C.
1	Commander Naval Missile Center ATTN: Mr. Lloyd O. Ritland, Code 3143 Point Mugu, California
1	Commander Air Force Systems Command ATTN: SCRS Andrews Air Force Base Washington 25, D. C.
1	Commander Electronic Systems Division ATTN: CCSIN (Spacetrack) L.G. Hanscom Field Bedford, Massachusetts
2	Commanding General Army Ballistic Missile Agency ATTN: Dr. C.A. Lundquist Dr. F.A. Speer Redstone Arsenal, Alabama
2	Director National Aeronautics and Space Administration ATTN: Dr. Robert Jastrow Mr. John T. Mengel 1520 H Street, N.W. Washington 25, D.C.
1	Chief of Staff, U.S. Army Research and Development ATTN: Director/Special Weapons Missiles & Space Division Washington 25, D.C.
1	Electrac Space Electronics Laboratory 537 B West Valencia Fullerton, California
1	International Business Machine Corp. Federal Systems Division ATTN: Mr. D.C. Eising - Systems Development Library 7230 Wisconsin Avenue Bethesda, Maryland
1	Philco Corporation Western Development Laboratory ATTN: Mr. Peter L. Berg 3875 Fabian Way Palo Alto, California

DISTRIBUTION LIST

No. of Copies	Organization
1	Space Technology Laboratories, Incorporated Information Services Acquisition Airport Office Building 8929 Sepulveda Boulevard Los Angeles 45, California
1	Westinghouse Electric Corporation Friendship International Airport ATTN: Mr. F.L. Rees - Mail Stop 649 P.O. Box 1697 Baltimore 3, Maryland
1	Mr. Edwin C. Adams Cook Electric Company Cook Technological Center 6401 Oakton Street Morton Grove, Illinois
1	Dr. O.J. Baltzer, Technical Director Textron Corporation Box 9207 Austin 17, Texas
1	Mr. W.J. Botha c/o N. I. T. R. P.O. Box 10319 Johannesburg, South Africa
1	Dr. R.N. Buland Ford Motor Company Aeronutronic Division System Analysis Department Ford Road Newport Beach, California
1	Mr. David M. Chase TGR Incorporated 2 Aerial Way Syosset, Long Island, New York
1	Dr. G.M. Clemence U.S. Naval Observatory Washington 25, D. C.
1	Mr. Arthur Eckstein U.S. Army Signal Research and Development Laboratory Astro-Electronics Division Fort Monmouth, New Jersey
1	Dr. Roger Gallet National Bureau of Standards Central Radio Propagation Lab. Boulder, Colorado
1	Dr. Wm. H. Guier Howard County Laboratory Applied Physics Laboratory Silver Spring, Maryland
1	Professor Robert A. Helliwell Stanford University Electronics Building Stanford, California
1	Dr. Paul Herget University of Cincinnati Cincinnati, Ohio
1	Mr. L. Lambert Columbia University 632 W. 125th Street New York 27, New York
1	Dr. A.J. Mallinckrodt 14141 Stratton Avenue Santa Ana, California
1	Mr. D.J. Mudgway Electronic Techniques Group Weapons Research Establishment P.O. Box 1424 H Salisbury, South Australia
1	Mr. T.W. O'Brien Radio Corporation of America Servo Sub-Unit Location 101-203 Moorestown, New Jersey

DISTRIBUTION LIST

No. of Copies	Organization
1	Mr. B. L. Rhodes Midwest Research Institute 425 Volker Boulevard Kansas City 10, Missouri
1	Dr. Thomas P. Rona Boeing Airplane Company Aero-Space Division Org. 2-5410, Mail Stop 22-99 P. O. Box 3707 Seattle 24, Washington
1	Professor William J. Ross Associate Professor of Electrical Engineering The Pennsylvania State University University Park, Pennsylvania
1	Mr. William Scharfman Stanford Research Institute Antenna Laboratory Menlo Park, California
1	Mr. E. H. Sheftelman AVCO Manufacturing Corporation Research and Advanced Development Division 201 Lowell Street Wilmington, Massachusetts
1	Professor George W. Swenson, Jr. University of Illinois Department of Electrical Engineering Urbana, Illinois
1	Dr. V. G. Szebehely General Electric Company Missile and Ordnance Systems Department 3198 Chestnut Street Philadelphia, Pennsylvania
1	Dr. James W. Warwick University of Colorado High Altitude Observatory Boulder, Colorado
1	Dr. Fred L. Whipple Smithsonian Institute Astrophysical Observatory 60 Garden Street Cambridge 38, Massachusetts

AD Accession No. UNCLASSIFIED

Ballistic Research Laboratories, APG
DETERMINATION OF ORBITAL ELEMENTS AND REFRACTION EFFECTS FROM SINGLE PASS DOPPLER OBSERVATIONS
R. B. Patton, Jr. and V. W. Richard

BRL Memo Report No. 1357 June 1961

DA Proj No. 503-06-011, OMSC No. 5010.11.143
UNCLASSIFIED Report

Doppler tracking systems - Design
Radar tracking - Satellites
Satellites - Detection

This report presents a method for the determination of the orbital elements of a satellite by observing, in the course of a single pass, the Doppler shift in the frequency of a radio signal which is either transmitted or reflected from the satellite. The method of solution consists of applying a series of differential corrections to a compatible set of approximations for the initial position and velocity components. Techniques for determining these approximations with sufficient accuracy to initiate the computation are discussed.

The method was developed for the DOPLOC tracking system which employs a narrow bandwidth, phase-locked, tracking filter. The latter has been designed to minimize random errors in Doppler frequency measurements derived from weak signals transmitted over extreme ranges.

Use is also made of satellite Doppler data to determine the total electron content in the ionosphere. A technique for measuring the dispersive Doppler effect is described. Results of computations with actual field data are presented.

AD Accession No. UNCLASSIFIED

Ballistic Research Laboratories, APG
DETERMINATION OF ORBITAL ELEMENTS AND REFRACTION EFFECTS FROM SINGLE PASS DOPPLER OBSERVATIONS
R. B. Patton, Jr. and V. W. Richard

BRL Memo Report No. 1357 June 1961

DA Proj No. 503-06-011, OMSC No. 5010.11.143
UNCLASSIFIED Report

Doppler tracking systems - Design
Radar tracking - Satellites
Satellites - Detection

This report presents a method for the determination of the orbital elements of a satellite by observing, in the course of a single pass, the Doppler shift in the frequency of a radio signal which is either transmitted or reflected from the satellite. The method of solution consists of applying a series of differential corrections to a compatible set of approximations for the initial position and velocity components. Techniques for determining these approximations with sufficient accuracy to initiate the computation are discussed.

The method was developed for the DOPLOC tracking system which employs a narrow bandwidth, phase-locked, tracking filter. The latter has been designed to minimize random errors in Doppler frequency measurements derived from weak signals transmitted over extreme ranges.

Use is also made of satellite Doppler data to determine the total electron content in the ionosphere. A technique for measuring the dispersive Doppler effect is described. Results of computations with actual field data are presented.

AD Accession No. UNCLASSIFIED

Ballistic Research Laboratories, APG
DETERMINATION OF ORBITAL ELEMENTS AND REFRACTION EFFECTS FROM SINGLE PASS DOPPLER OBSERVATIONS
R. B. Patton, Jr. and V. W. Richard

BRL Memo Report No. 1357 June 1961

DA Proj No. 503-06-011, OMSC No. 5010.11.143
UNCLASSIFIED Report

Doppler tracking systems - Design
Radar tracking - Satellites
Satellites - Detection

This report presents a method for the determination of the orbital elements of a satellite by observing, in the course of a single pass, the Doppler shift in the frequency of a radio signal which is either transmitted or reflected from the satellite. The method of solution consists of applying a series of differential corrections to a compatible set of approximations for the initial position and velocity components. Techniques for determining these approximations with sufficient accuracy to initiate the computation are discussed.

The method was developed for the DOPLOC tracking system which employs a narrow bandwidth, phase-locked, tracking filter. The latter has been designed to minimize random errors in Doppler frequency measurements derived from weak signals transmitted over extreme ranges.

Use is also made of satellite Doppler data to determine the total electron content in the ionosphere. A technique for measuring the dispersive Doppler effect is described. Results of computations with actual field data are presented.

AD Accession No. UNCLASSIFIED

Ballistic Research Laboratories, APG
DETERMINATION OF ORBITAL ELEMENTS AND REFRACTION EFFECTS FROM SINGLE PASS DOPPLER OBSERVATIONS
R. B. Patton, Jr. and V. W. Richard

BRL Memo Report No. 1357 June 1961

DA Proj No. 503-06-011, OMSC No. 5010.11.143
UNCLASSIFIED Report

Doppler tracking systems - Design
Radar tracking - Satellites
Satellites - Detection

This report presents a method for the determination of the orbital elements of a satellite by observing, in the course of a single pass, the Doppler shift in the frequency of a radio signal which is either transmitted or reflected from the satellite. The method of solution consists of applying a series of differential corrections to a compatible set of approximations for the initial position and velocity components. Techniques for determining these approximations with sufficient accuracy to initiate the computation are discussed.

The method was developed for the DOPLOC tracking system which employs a narrow bandwidth, phase-locked, tracking filter. The latter has been designed to minimize random errors in Doppler frequency measurements derived from weak signals transmitted over extreme ranges.

Use is also made of satellite Doppler data to determine the total electron content in the ionosphere. A technique for measuring the dispersive Doppler effect is described. Results of computations with actual field data are presented.